12-2015

A Simulation Platform for Accurate Prediction of In-bin Drying and Storage of Rough Rice

Houmin Zhong
University of Arkansas, Fayetteville

A Simulation Platform for Accurate Prediction of In-bin Drying and Storage of Rough Rice

A thesis submitted in partial fulfillment
of the requirements for the degree of
Master of Science in Food Science

by

Houmin Zhong
University of California, Davis
Bachelor of Science in Biological Systems Engineering, 2013

December 2015
University of Arkansas

This thesis is approved for recommendation to the Graduate Council.

_____
Dr. Griffiths G. Atungulu
Thesis Director

_____
Dr. Andronikos Mauromoustakos
Committee Member

_____
Dr. Scott Osborn
Committee Member

_____
Dr. Terry Siebenmorgen
Committee Member

ABSTRACT

Natural air (NA), in-bin drying and storage of rough rice generally maintains high grain quality, but the associated slow movement and occasional stagnation of the drying front during the process may result in problems of rice quality reduction, mold growth, and mycotoxin development, especially for rough rice in the top layers of the bin. Using modeling techniques to simulate in-bin rough rice drying in typically-encountered field scenarios may provide a tool for rapidly predicting the grain condition as drying progresses. The objectives for this study were to (1) investigate accurate models for predicting equilibrium moisture content (EMC) of rough rice at set conditions of air temperature and relative humidity (RH), (2) develop and validate a mathematical model for predicting moisture content (MC) and temperature profiles of rough rice during NA, in-bin drying, and (3) perform computer simulations using the developed mathematical model to determine the impacts of drying strategy (rough rice initial MC, drying-start date, air flowrate, and fan control strategy) on rough rice drying duration, maximum dry matter loss, and percent overdrying. In order to accomplish objective (1), adsorption and desorption isotherms of long-grain hybrid rough rice at temperatures ranging from 15 ℃ to 35 ℃ and RHs of 10% to 90% were determined by using a Dynamic Vapor Sorption analysis device. Non-linear fitting techniques were used to determine constants of models for predicting rough rice adsorption or desorption EMCs. It was determined that the modified Halsey and modified Chung-Pfost equations were the best models to describe rough rice adsorption and desorption isotherms, respectively (RMSEs = 0.54% MC in dry basis and 0.91% MC in dry basis, respectively). To achieve objective (2), Post-Harvest Aeration Simulation Tool - Finite Difference Method, developed by Bartosik and Maier (2004), was modified for rice and used to simulate in-bin rough rice drying in Arkansas. Simulation results were validated by field

experiments, which used modern, on-farm bins equipped with "cabling and sensing technology" for in-bin RH and rough rice temperature measurement; the rough rice MC was calculated based on the measured RH and temperature data. The sensor-determined data and simulation results of MC and temperature were compared. The simulation results described well the general trends of rough rice MC and temperature profiles (for MC, mean RMSE = 0.56% MC in wet basis; for temperature, mean RMSE = 1.77 ℃). The study validated the accuracy of the developed simulation model for prediction of in-bin drying and storage of rough rice. In order to accomplish objective (3), simulations of in-bin drying of rough rice with different drying strategies was performed. A twenty-year weather data set (1995 to 2014) of ambient air temperature and RH of the U.S. Mid-South rice growing locations (Jonesboro, West Memphis, and Stuttgart, Arkansas, and Greenville and Tunica, Mississippi) were procured. Drying simulations were performed using air flowrates 0.55, 1.10, 1.65, and 2.20 m^3 $min\text{-}t^{-1}$, drying-start dates of 15 August, 15 September, and 15 October, and rough rice initial MCs of 16% to 22% (wet basis). Fan control strategies comprised running the drying fan continuously, at set window of natural air equilibrium moisture content, and air EMC window with supplemental heating option. Results showed that rough rice drying duration, dry matter loss, and percent overdrying were dependent on selected drying strategy with fan control strategy, initial rough rice MC, and air flowrate being key factors. Information generated using the simulations could guide rice producers, especially in selected U.S. Mid-South, to effectively dry rough rice in a timely manner, and mitigate problems of rice quality reduction, excessive mold growth, and mycotoxin contamination.

ACKNOWLEDGMENTS

Special thanks are extended to my advisor, Dr. Griffiths G. Atungulu of the University of Arkansas Division of Agriculture, Food Science Department, for all of his help with my thesis. His vast knowledge and guidance was key to my research and writing of this thesis. It would have been impossible to make it through my MS degree without his help. Also, special thanks goes out to the rest of my thesis committee members: Dr. Andronikos Mauromoustakos, Dr. Scott Osborn, and Dr. Terry Siebenmorgen for their insightful comments and support.

My sincere thanks also goes to the University of Arkansas Rice Processing Program for giving access to their research facilities. I thank my labmates in the University of Arkansas Grain Processing Program for all the fun we have had in the last two years. I must also acknowledge Chandra Singh of OPI-systems Inc. (Calgary, Alberta, Canada) and Mike Shook of Agri Process Innovations Inc. (Stuttgart, Arkansas, USA) for sharing useful information about rice temperature and moisture content, bin configurations, bin locations, and bin management history. I recognize that this research would not be possible without the support from rice producers in the Arkansas Delta and White River ecological zones, especially Mike Sullivan, Steven Henderson, and Paul McKinney, and the financial assistance of the Arkansas Rice Research and Promotion Board and the University of Arkansas Division of Agriculture. I sincerely express my gratitude to all those agencies and related parties.

Last but not the least, I would like to thank my family: my parents and my brother for their love and encouragement throughout my master degree and my life.

TABLE OF CONTENTS

1. INTRODUCTION 1

1.1 Problem identification 1

1.2 Equilibrium moisture content of rough rice 2

1.3 Natural air, in-bin drying 4

1.4 Modeling of in-bin drying 8

2. OBJECTIVES 11

3. MATERIALS AND METHODS 12

3.1 Equilibrium moisture content determination 12

3.2 Development of computer simulation platform and mathematical simulations 13

3.2.1 Development of user input-interface 19

3.3 Simulations for model validation 20

3.4 Simulations to assess impact of in-bin rough rice drying strategies 27

3.4 Statistical analysis 29

4. RESULTS AND DISCUSSION 31

4.1 Sorption isotherms estimation 31

4.2 Simulations for model validation 36

4.2.1 Meter-measured data vs. sensor-determined data 36

4.2.2 Sensor-determined data vs. simulation results 37

4.3 Simulations to assess impact of in-bin rough rice drying strategies 45

5. CONCLUSION AND FUTURE RESEARCH 55

5.1 Equilibrium moisture content determination 55

5.2 Simulations for model validation 55

5.3 Simulations to assess impacts of in-bin rough rice drying strategies 56

5.4 Future studies 58

REFERENCES 59

1. INTRODUCTION

1.1 Problem identification

In-bin drying and storage of rough rice using natural air (NA), if not managed properly, is prone to contamination of rough rice with mycotoxins (e.g., aflatoxin), posing significant public health risks and reducing overall rice quality. The NA drying method involves the use of a fan (often more than one) to mechanically push ambient air through a rough rice column, from the bottom to the top of the bin; as the air moves vertically through the rough rice column inside the bin, the air "quality" determines whether the rough rice gains or loses moisture. The air "quality", also referred to as the equilibrium moisture content (EMC), defines the capability of the rough rice to hold moisture at set conditions of air temperature and relative humidity (RH). Depending on local weather conditions, the duration required for NA, in-bin drying may not be conducive for timely and complete drying, especially for upper layers of rough rice (Atungulu, Zhong, Thote, Okeyo, & Couch, 2015). It is important to know the extent to which drying with NA in a particular location influences rough rice drying duration to mitigate rice quality reduction, mold growth, and development of mycotoxin.

A field study to obtain NA, in-bin drying kinetics for rough rice would require extensive, time-consuming, and costly experimentation. However, an accurate mathematical model may simplify prediction of the NA, in-bin drying process of rough rice. There is, therefore, a critical need to develop and validate an accurate model that could be used to simulate NA, in-bin drying of rough rice and the effects on rice quality. The model could be used for simulations to provide suitable drying conditions for rough rice at different geographical regions. In the absence of such a model to predict suitable drying strategies, in-bin rough rice drying and storage with NA will

be more susceptible to grain quality loss and contamination with toxigenic fungi and their associated mycotoxins, many of which are carcinogenic to humans.

1.2 Equilibrium moisture content of rough rice

Moisture content of rough rice plays an important role in drying, storage, milling, and end-use processing performance (Choi, Lanning, & Siebenmorgen, 2010). In rice drying, the EMC represents the MC that can be reached under a given condition of drying air temperature and RH. As such, the MC of grain in a bin, along with the air EMC associated with a particular grain, determine whether drying or rewetting occurs when air passes through the mass of grain. If the air EMC is less than the grain MC, the grain will dry – a phenomena referred to as desorption. If the air EMC is greater than the grain MC, the grain will rewet – a phenomena referred to as adsorption. The difference between desorption and adsorption isotherms is called hysteresis. Desorption EMCs are always greater than adsorption EMCs in the middle portion of the RH range, and the difference between them converges to zero at the least and greatest RHs (Brooker, Bakker-Arkema, & Hall, 1992; Choi et al., 2010).

Mathematical models for estimating the EMC of grains such as rough rice are listed in ASABE Standard D245.6 (ASABE Standards, 2012). The modified Chung-Pfost, modified Halsey, modified Henderson, and modified Oswin equations can be used to describe the EMC of grains with sets of predetermined empirical constants in desorption and adsorption phenomena (table 1.1). Many studies on EMC isotherms of rice have been done (Banaszek & Siebenmorgen, 1990; Iguaz & Virseda, 2007; Ondier, Siebenmorgen, Bautista, & Mauromoustakos, 2011). Ondier et al. (2011) rewetted or dried long-grain hybrid rough rice with 11.6% initial MC (IMC) (all MCs are expressed on a wet basis (w.b.) unless specified otherwise) at temperatures of 10 ℃,

20 ℃, 30 ℃, 45 ℃, or 60 ℃ and 10% to 70% RH, but the reported isotherms did not document the hysteresis effects. Iguaz and Versada (2007) dried medium-grain rough rice with 14.5% IMC at temperature of 40 ℃ to 80 ℃ and 15% to 85% RH, but the temperature range was above the typical NA drying temperature range (below 40 ℃ (figure 4.5)). Banaszek and Siebenmorgen (1990) rewetted rice at temperature of 12.5 ℃, 15 ℃, 20 ℃, or 30 ℃ and 70% to 90% RH, but the RH range only covers the upper part of typical NA drying RH range. Since none of the above findings showed both adsorption and desorption isotherms in NA drying temperature range for rough rice, a new study was needed to accurately predict the rough rice MC during in-bin drying. The results reported by foregoing authors were generated using the traditional methods in which samples were placed in desiccators or air-circulating chambers. With the preceding methods, samples may take several weeks to reach equilibrium in desiccators, or high air flowrate may affect the accuracy of data obtained from the weight-measuring equipment. A new method (Dynamic Vapor Sorption (DVS)), which utilizes low airflow inside the chamber, accurate RH control, and an accurate weighing balance was used in this study, instead of the traditional methods.

Dynamic Vapor Sorption is a gravimetric method that measures how much of a solvent, such as water, is absorbed by a sample. Compared to the traditional saturated salt solution method, the DVS method uses a mixture of saturated water vapor and dried air to accurately control RH levels in a sealed chamber. When DVS is used, the fast equilibration duration between the sample and air can reduce sample respiration and mold growth on the sample. The method also uses an ultra-sensitive recording microbalance which improves the accuracy of weight change of the sample (Bingol, Prakash, & Pan, 2012). The DVS method is equipped with a chilled mirror hygrometer humidity sensor for accurate measurement of air RH. The DVS

method has been used in the pharmaceutical industries with success (Hogan & Buckton, 2001; Baumgartner, Kristl, & Peppas, 2002; Agrawal, Manek, Kolling, & Neau, 2004; Young, et al., 2007). In recent years, the DVS method has found applications for measurement of isotherms of different food materials (Teoh, Schmidt, Day, & Faller, 2001; Guillard, Broyart, Bonazzi, Guilbert, & Gontard, 2003; Roman-Gutierrez, Mabille, Guilbert, & Cuq, 2003; Bingol et al., 2012). Bingol et al. (2012) preformed a study to compare isotherms obtained using the DVS method and saturated salt solution methods for rough rice at 25 ℃ and 0 to 100% RH; the authors recommended the DVS method for materials with low diffusion coefficients, such as rough rice.

Table 1.1. Moisture sorption prediction models[1]

Name of Model	Equation[2]
Modified Chung-Pfost	$MC \times 100 = -\frac{1}{\mathrm{B}}\ln\left[-\frac{(T+\mathrm{C})\,ln(RH)}{\mathrm{A}}\right]$
Modified Halsey	$MC \times 100 = \left[-\frac{\exp(\mathrm{A}+\mathrm{B}*T)}{\ln(RH)}\right]^{\frac{1}{\mathrm{C}}}$
Modified Henderson	$MC \times 100 = \left[\frac{\ln(1-RH)}{-\mathrm{A}*(T+\mathrm{C})}\right]^{\frac{1}{\mathrm{B}}}$
Modified Oswin	$MC \times 100 = (\mathrm{A}+\mathrm{B}*T)\left(\frac{1-RH}{RH}\right)^{\frac{-1}{\mathrm{C}}}$

[1]ASABE Standard D245.6 (2012)
[2]*MC* is air equilibrium moisture content in decimal dry basis; *RH* is relative humidity expressed as a decimal; *T* is temperature (℃); and A, B, and C are empirical constants.

1.3 Natural air, in-bin drying

Figures 1.1 (a) and (b) show a photo and a schematic of an in-bin grain dryer, respectively. The dryer uses NA or slightly heated air at 3 ℃ to 8 ℃ above ambient (Brooker et

al., 1992). A typical in-bin grain dryer has perforated floor, one or more drying fan(s), grain spreader, and exhaust vents (figure 1.1(b)). The low temperature, relatively slow air flowrate (from 0.69 to 2.77 m^3 $min\text{-}t^{-1}$) associated with NA drying are generally known to prevent rice kernel fissuring and reduction in rice milling quality, especially head rice yield (HRY) (Cnossen, Siebenmorgen, Yang, & Bautista, 2001; Inprasit & Noomhorm, 2001; Ondier, Siebenmorgen, & Mauromoustakos, 2010; Ambardekar & Siebenmorgen, 2012). Preventing HRY reduction during drying is very critical and has significant economic importance for the rice industry (Cnossen & Siebenmorgen, 2000). Additional advantages of the NA, in-bin drying practice in the rice industry include enabling identity preservation of rice for specific market niches, flexibility to market rice at a time when maximum profitability is attainable, and increasing the drying capacity to avoid bottlenecks at commercial dryer facilities during peak harvest seasons.

(a)

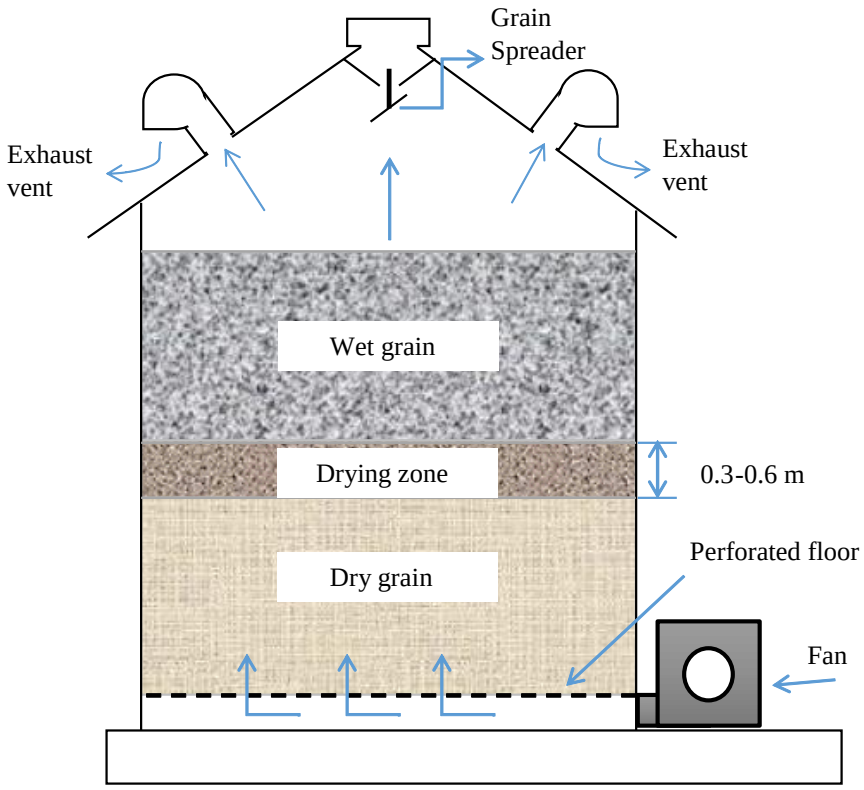

(b)

Figure 1.1. Natural air, in-bin drying bin diagrams (a) a photo of actual bins; (b) schematic of a single bin.

The duration required to dry rough rice in a bin to targeted MC depends on the local weather (temperature and RH), air flowrate, fan control strategy, drying-start date, and IMC of the rice. The combinations of these factors can be controlled to create drying strategies. The drying strategies used may affect rice quality indices, including HRY, milled rice color, mold growth, and germination percentage (Sahay & Gangopadhyay, 1985; Tirawanichakul, Prachayawarakorn, Tungtrakul, Chaiwatpongskorn, & Soponronnarit, 2003; Schluterman & Siebenmorgen, 2004).

In-bin drying can be accomplished through (1) uncontrolled drying and (2) EMC-controlled drying modes of fan operation. Under the uncontrolled drying mode, the bin fan is

operated continuously until the grain dries to safe storage MC. Periods of extreme drying and rewetting are common, which increase the fan running duration, and consequently, result in greater fan operational costs. Also, if overdrying of rice occurs followed by rapid rewetting, fissuring of rice kernels due to rapid moisture adsorption may occur, resulting in reduced HRY (Siebenmorgen & Jindal, 1986).

Recently-introduced "cabling and sensing technology" for use in NA drying bins allows monitoring of rough rice MC and automated fan control during drying and storage (Singh, Jayas, & Larson, 2014) which is referred to as EMC-controlled drying. Modern drying bins are equipped with cables (with sensors for grain temperature and air RH), plenum temperature, RH, and pressure sensors, headspace temperature and RH sensors, pitfall traps for insects, and a weather station. These devices communicate to a grain management software through wired or wireless communication thereby allowing the capability to monitor rough rice temperature and MC during drying. Decisions to turn the fan on or off are based on real time conditions of drying air EMC and temperature and rough rice MC and temperature. When the fan is turned on, drying air is pushed through rough rice in the bin thereby absorbing moisture from the rice (may add moisture to the rice if EMC of air is greater than MC of rice). The air moves upwards to the top where it exits the bin from the exhaust vents.

The features of the modern bins allow the fan to be operated only under set conditions thereby minimizing overdrying or rewetting of rough rice. Some producers have bins equipped with low temperature heaters, such as gas burners or electric resistance heaters. The heaters are used to lower air EMC and increase the moisture removal rate during drying (Brooker et al. 1992). In practice, the maximum and minimum EMC limits of inlet air are regulated to reduce energy consumption or reduce the drying duration. The minimum EMC for fan operation can be

fixed or changed as drying progresses.

A problem with NA drying and lower drying rate can be failure of rice to dry adequately resulting in development of molds in the bins. From consumer and producer standpoints, the potential of mold growth that can lead to mycotoxin production on rice presents the greatest human health-related problem. Mycotoxins, especially aflatoxin, are known carcinogens that pose severe health hazards to consumers of grains and co-products. Even trace quantities of rice contamination with aflatoxin could lead to rejection of entire bins of rice and cause significant economic loss to producers (Richard, et al., 2003). At present, the United States Food and Drug Administration (FDA) regulates the level of aflatoxin at 20 ppb or less for grain destined for human consumption. It is vital that the in-bin drying strategy adopted for a particular locality prevents the production of mycotoxin on rice, and arrest excessive rice respiration, which leads to mold growth and dry matter loss (DML) of the grain (Seib, Pfost, Sukabdi, Rao, & Burroughs, 1980).

1.4 Modeling of in-bin drying

Logarithmic, non-equilibrium, and equilibrium models have been used to predict grain drying characteristics. The non-equilibrium and logarithmic models can be applied in all grain drying systems (Pabis, Jayas, & Cenkowski, 1998; Ekechukwu & Norton, 1999). The non-equilibrium modeling approach assumes that the drying air and the grain would not reach equilibrium in a given time interval; sets of partial differential equations are derived from the laws of heat and mass transfer, and the mathematical theory of drying single solid bodies (Srivastava & John, 2002). The logarithmic model describes deep-bed drying under uniform initial and constant boundary conditions (Barre, Baughman, & Hamdy, 1971). The logarithmic

model provides an explicit analytical solution of drying duration as a function of drying air parameters, and grain properties (Aregba & Nadeau, 2007). The typical air flowrate used during rough rice drying in NA bin systems is less than 2.77 m^3 $min\text{-}t^{-1}$ (2 cfm bu^{-1}). With low temperature and low air flow rate, the drying air can be assumed to reach equilibrium in each layer of rice in the bin during a given time interval. Compared to the non-equilibrium and logarithmic models, equilibrium models have fast computation time (Sharp, 1982).

Several authors have modified the equilibrium models of Bloome and Shove (1971) and Thompson (1972) to improve their accuracy for temperature and MC predictions during NA rice drying (Sharma & Muir, 1974; Mittal & Otten, 1982; Soponronnarit, 1988; Jindal & Siebenmorgen, 1994; Saksena, Montross, & Maier, 1998; Bartosik & Maier, 2004). Jindal and Siebenmorgen (1994) improved and validated Thompson's equilibrium model (1972) for rice with experimental data and concluded that this model predicted grain temperature and MC with reasonable accuracy. Saksena et al., (1998) developed nine in−bin fan control strategies using a finite-difference method based on an equilibrium model; this resulted in a program termed the Post-Harvest Aeration Simulation Tool - Finite Difference Method (PHAST-FDM). Bartosik and Maier (2004) developed and simulated different fan control strategies using the PHAST-FDM program for in-bin drying of corn. With modern computational technology, a program, which was built on an equilibrium model, can be used to assess the impacts on NA rice drying with different combinations of drying strategies.

Singh et al. (2014) reported on simulations to assess fan control options during NA, in-bin drying of wheat in Canadian Prairies and provided optimal fan control strategies that minimized wheat spoilage. Lawrence, Atungulu, and Siebenmorgen (2015) performed a similar study on rough rice in Arkansas and gave suggestions on suitable air flowrates and fan control

strategies based on drying cost and drying duration. The type of fan control strategy, applied air flowrate, and drying-start date play major roles to dictate what the upper limit of IMC of rough rice should be to minimize rice quality reduction at a geographic location. The application of mathematical models and computer simulation is therefore useful in predicting in-bin drying performance in a particular geographic location.

2. OBJECTIVES

The objectives for this research were to investigate the effectiveness of using mathematical modeling approaches to simulate NA, in-bin drying of rice, and provide suitable drying strategies that maintain rough rice quality. The specific objectives for this study were as follow:

1) Investigate accurate models for predicting EMC of rough rice at set conditions of air temperature and RH.
2) Develop and validate a mathematical model for predicting MC and temperature profiles of rough rice during NA, in-bin drying in Arkansas.
3) Perform computer simulations using the developed mathematical model to determine the impacts of rough rice IMC, drying-start date, air flowrate, and fan control strategy on rice drying duration, maximum DML, and percent overdrying at different rice-growing locations in the U.S. Mid-South.

3. MATERIALS AND METHODS

3.1 Equilibrium moisture content determination

Long-grain rice cultivar Clearfield^{TM} (CL) XL745, grown at Newport, Arkansas, was harvested in fall of 2014 at 16% MC. Immediately after harvest, rough rice samples were placed in sterile polyethylene bags, sealed, and stored in a cooler set at 4 ℃. The samples were stored in the cooler and retrieved later for experiments. To determine the IMC of rice, samples from the bags were retrieved and allowed to equilibrate at room conditions, and then 15 g of the sample was placed into a conductive oven set at 130 ℃ (Shellblue, Sheldon Mfg., Inc., Cornelius, Oreg.). The sample was kept in the oven for 24 hours, after which it was removed, placed in the desiccator, and allowed to cool for at least half an hour (Jindal & Siebenmorgen, 1987).

The adsorption and desorption isotherms of the rough rice samples at IMC of 16% were determined using a DVS analysis equipment (AquaLab Vapor Sorption Analyzer (VSA), Decagon Devices, Inc., Pullman, Wash.). Stainless steel cup, filled with 2 g of rough rice, was placed into the VSA chamber which was set to target temperatures 15 ℃, 25 ℃, or 35 ℃ and RHs at 10%, 30%, 50%, 70%, and 90%. The VSA automatically recorded the rough rice weight changes at the set conditions, and equilibrium of the sample with the air was determined when the weight difference between two successive readings of the sample weight was less than 0.01% in one hour. Using the predetermined original rough rice IMC, the rough rice EMCs at various RHs and temperatures were calculated for both adsorption and desorption conditions. The experiments were done in triplicate.

3.2 Development of computer simulation platform and mathematical simulations

A computer simulation program (PHAST-FDM), written in Visual Basic.NET (Microsoft Corp., Redmond, Wash.), was modified for use with rough rice. The program was used to simulate NA, in-bin drying of rough rice at representative rice-growing locations. Modifications of the program included development of an interactive Graphical User Interface (GUI), incorporation of updated EMC models of rough rice, addition of functions to calculate percent overdrying and rice DML, and addition of multiple options for controlling when to end the simulations. The model used for in-bin drying simulations was based on the following assumptions:

1) In each layer, energy and moisture of rough rice and air reach equilibrium in a given time interval.
2) Heat and mass transfer between the air and the rough rice are adiabatic.
3) There is negligible heat loss through the bin wall.
4) The initial temperature and MC of rough rice in each layer, inlet air temperature and RH throughout the drying period, and other input parameters (drying-start date, bin dimensions, air flowrate, simulation ending condition, and fan control strategy) are known.

The energy balance applied to a thin rice layer was determined as described by Jindal and Siebenmorgen (1994):

$$c_a T_o + H_o(h_v + c_v T_o) + c_g G_o r + c_w G_o\left(H_f - H_o\right) = c_a T_f + H_f\left(h_v + c_v T_f\right) + c_g T_f r \qquad (1)$$

where, c_a – specific heat of dry air (J (kg of dry air)$^{-1}$ K^{-1}); c_g – specific heat of grain (J (kg of wet grain)$^{-1}$ K^{-1}); c_v – specific heat of water vapor (J (kg of water vapor)$^{-1}$ K^{-1}); c_w – specific

heat of water (J (kg of water in grain)$^{-1}$ K^{-1}); H_o – absolute humidity of air entering the control volume ((kg of water) (kg of dry air)$^{-1}$); H_f – absolute humidity of air leaving the control volume ((kg of water) (kg of dry air)$^{-1}$); T_o – initial air temperature (^{o}C); T_f – final air and grain temperature (^{o}C); h_v – latent heat of vaporization of water (J (kg of water vapor)$^{-1}$); G_o – initial grain temperature (^{o}C); and r – grain mass to dry air ratio ((kg of wet grain) (kg of dry air)$^{-1}$).

On the left side of equation 1, the first term represents the energy of the dry air with respect to 1 kg of dry air before air entering the rough rice layer, and the second term represents the energy of the water vapor in the air with respect to 1 kg of dry air before air entering the rough rice layer; also, the third term represents the energy of the wet rough rice layer (with a fix percentage of water) with respect to 1 kg of dry air before air entering the rough rice layer. It is assumed that the change of the water in the rough rice is equal to the change of humidity in the air; therefore, the fourth term represents the energy difference of the water which is desorbed or adsorbed by the rough rice with respect to 1 kg of dry air. The three terms on the right side of equation 1 correspond to the first three terms of the left side of the equation, and they are for conditions after the air exits the rough rice layer.

The moisture balance applied to a thin rice layer, with the assumption that the mass of water evaporated from the rough rice in the layer is equal to the change in mass of water vapor in the air passing through the layer, was determined as described by Jindal and Siebenmorgen (1994):

$$H_f - H_o = \left(MC_o - MC_f\right) r/100 \tag{2}$$

$$r = (\rho_g \, d_x)/(\rho_a v_a t) \tag{3}$$

where, MC_o – initial MC of grain in percentage wet basis; MC_f – final MC of grain in percentage wet basis; t – time interval (s); ρ_a – density of air ((kg of air) m^{-3}) ; ρ_g – density of

grain ((kg of wet grain) m^{-3}); v_a– velocity of air (m s^{-1}); and d_x – layer thickness (m).

Using the exiting air RH and temperature, the rough rice MC in each layer at the end of a time step was determined. The modified Chung-Pfost equation (equation 4) with constants specified for long-grain hybrid rough rice in adsorption and desorption conditions was used:

$$MC_e = -\frac{1}{\mathrm{B}}\ln\left[\frac{-(T+\mathrm{C})\ln(RH)}{\mathrm{A}}\right] \quad (4)$$

where, MC_e – equilibrium moisture content in percentage dry basis; RH – relative humidity in decimal; T – temperature (℃); A, B, and C are empirical constants.

Adsorption and desorption constants (two sets of A, B, and C) for equation 4 were determined in this study for long-grain hybrid rice cultivar (CL XL745). RH, temperature, and partial and saturated vapor pressures of air were determined thus (ASABE Standards, 2014):

$$RH = \frac{P_v}{P_s} \quad (5)$$

$$P_v = \frac{101325\,H}{0.6219 + H} \quad (6)$$

$$P_s = \mathrm{K} \times \exp\left(\frac{\mathrm{A} + \mathrm{B}\,T + \mathrm{C}\,T^2 + \mathrm{D}\,T^3 + \mathrm{E}\,T^4}{\mathrm{F}\,T - \mathrm{G}\,T^2}\right) \quad (7)$$

where, RH – air relative humidity in decimal; P_v – partial vapor pressure of air (Pa); P_s – saturated vapor pressure of air (Pa); H – absolute humidity of air ((kg of water) (kg of dry air)$^{-1}$); T – air temperature (℃); K = 22105649.25; $\mathrm{A} = -27405.526$; $\mathrm{B} = 97.5413$; $\mathrm{C} = -0.146244$; $\mathrm{D} = 0.12558 \times 10^{-3}$; $\mathrm{E} = -0.48502 \times 10^{-7}$; $\mathrm{F} = 4.34903$; $\mathrm{G} = 0.39381 \times 10^{-2}$.

Using equations 1 to 7, the temperature and RH of air exiting each rough rice layer and the rough rice temperatures at the end of each time step were determined. Finite difference method was used to determine the time-step solutions of rough rice MC and temperature as well

as the intake and exit air conditions in successive layers of the rough rice inside the bin. The column of rough rice inside the bin was divided into N thin layers (N = 20). The depth of each layer of rough rice (d_x) in this study was equal to the column height divided by the number of layers. The finite difference method illustrated in figure 3.1 is a two dimensional figure with number of times on the x-axis and layers on the y-axis. The model assumed fixed volume of air with constant air velocity passed into the drying bin, through N layers of rough rice, reaching to the top, and exiting the bin for j times. For instance, initial conditions of rough rice temperature GT(n,1) and moisture content M(n,1), for n ϵ (1,N) and initial air conditions of temperature AT(1,j) and absolute humidity AX(1,j), for j ϵ (1,J) are known, so other layer conditions could be calculated, thus: when air (AT(1,1) and AX(1,1)) passes through the first layer of rough rice for the first time, the rough rice layer conditions change from the initial conditions (M(1,1) and GT(1,1)) to equilibrium conditions (M(1,2) and GT(1,2)), and the air conditions also change from the inlet air conditions to the outlet conditions AT(2,1) and AX(2,1), which are the initial inlet air conditions of the second layer of rough rice. Similarly, when air (AT(2,1) and AX(2,1)) passes through the second layer for the first time, the second layer conditions change from M(2,1) and GT(2,1) to M(2,2) and GT(2,2), the air conditions also change from the inlet air conditions to the outlet conditions (AT(3,1) and AX(3,1)). This process is repeated until the first time N^{th} layer rough rice conditions (M(N,2) and GT (N,2)) and outlet air conditions (AT(N+1,1) and AX(N+1,1)) are known. Next, as second time air (AT(1,2) and AX(1,2)) passes through the first layer, the rough rice layer conditions change from the initial conditions (M(1,2) and GT(1,2)) to equilibrium condition (M(1,3) and GT(1,3)), and the air conditions also change from the inlet air conditions to the outlet conditions AT(2,2) and AX(2,2) which is the inlet air conditions of second layer of rough rice for the second time. This step is repeated until N^{th} layer rough rice

condition for the second time M(N,3) and GT(N,3) and outlet air conditions (AT(N+1,2) and AX(N+1,2)) are determined. Consequently, after third time air passes through all the rough rice layers, the conditions of rough rice (M(n,4) and GT(n,4), for n ϵ (1,N)) and all outlet air conditions (AT(n,3) and AX(n,3), for n ϵ (2,N+1)) are determined. By repeating these calculations step-wise, the conditions for all rough rice layers (M(n,j) and GT(n,j), for n ϵ (1,N) and j ϵ (2,J+1)) and all outlet air conditions of the layers (AT(n,j) and AX(n,j), for n ϵ (2,N+1) and j ϵ (1,J)) were determined.

The DML equation in the PHAST-FDM program was modified based on Seib et al. (1980) for rough rice. The DML equation used is:

$$DML = 1 - exp[-\mathrm{A}t^{\mathrm{B}} exp(\mathrm{C}(T - 15.6) + \mathrm{D}(MC - 0.14))] \quad (8)$$

where, *DML* – dry matter loss in decimal; *t* – storage duration (h 1000^{-1}); *T* – temperature (^{o}C); *MC* – moisture content in decimal wet basis; A, B, C, and D are listed in table 3.1 (Seib et al., 1980).

Table 3.1. Constants of dry matter loss equation (equation 8) used for rough rice. Taken from Seib et al. (1980).

Grain Type	A	B	C	D
Long-grain	0.00189	0.654	0.068	33.61
Medium-grain	0.00091	0.710	0.049	31.62

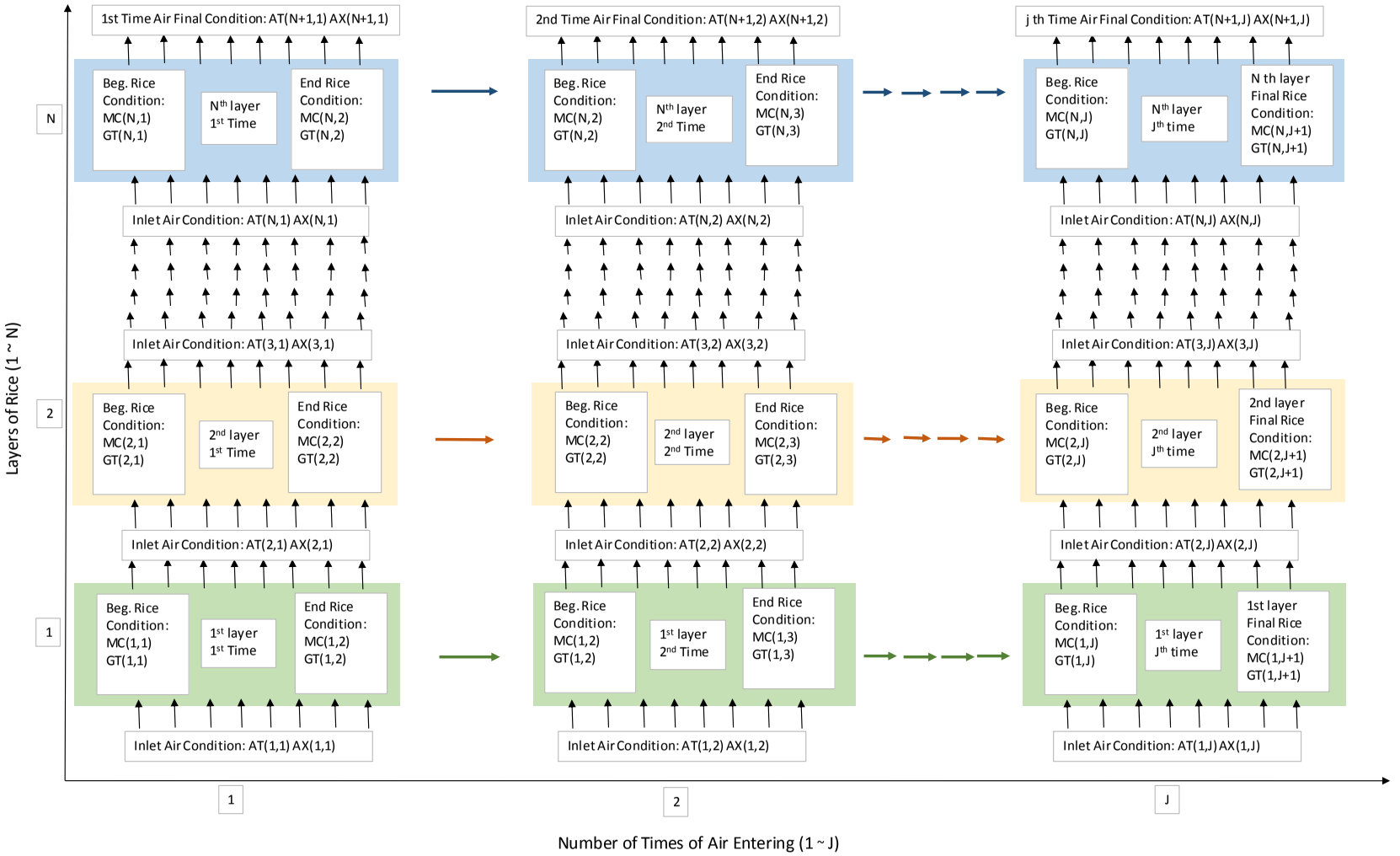

Figure 3.1. A finite difference routine used to determine the time–step solutions of rough rice moisture content and temperature (from beginning (beg.) conditions to end conditions) as well as the inlet and exit air conditions in the successive layers of rough rice inside the bin.

3.2.1 Development of user input-interface

A user-friendly interface that was developed for the program used in the simulation is shown in figure 3.2. The interface provides for selecting (1) fan control strategy, (2) bin configuration, (3) simulation date, (4) rice initial MC and temperature conditions, (5) simulation ending criteria, etc. The fan control strategies comprise of running the fan continuously which is shown as “Continuous natural air” in the user interface, during the day “Natural air day only”, during the night “Natural air night only”, at set windows of drying air EMC without supplemental heating option “EMC controlled natural air”, and at set windows of drying air EMC with supplemental heating option “EMC controlled air with supplemental heat”. Bin configurations include bin size and air flowrate. The program user could change initial temperature and IMC of each layer of rough rice and drying-start date. The interface allows the user to select presetted harvest location, grain type, and one or more of six different simulation ending criteria. The ending criteria are when (1) target average MC of dried rough rice falls below a specified MC which is shown as “Ave MC” in the user interface; (2) top layer MC of rough rice falls below a specified MC “Top layer MC”; (3) maximum DML of rough rice exceeds a specified percentage “Dry matter loss”; (4) simulation runs until a specific date “Fixed date”; (5) simulations runs until a fixed rice drying duration is achieved “# of days”; and (6) average temperature of rough rice exceeds a specified temperature “Temperature”. For example, the settings in figure 3.2 indicate that the simulation will end when top layer of rough rice dries below 14% MC or the drying duration reaches 90 days. To accurately calculate energy consumption and drying cost, the user has to enter fan and heater efficiencies, grain value, and the costs of electricity and propane gas.

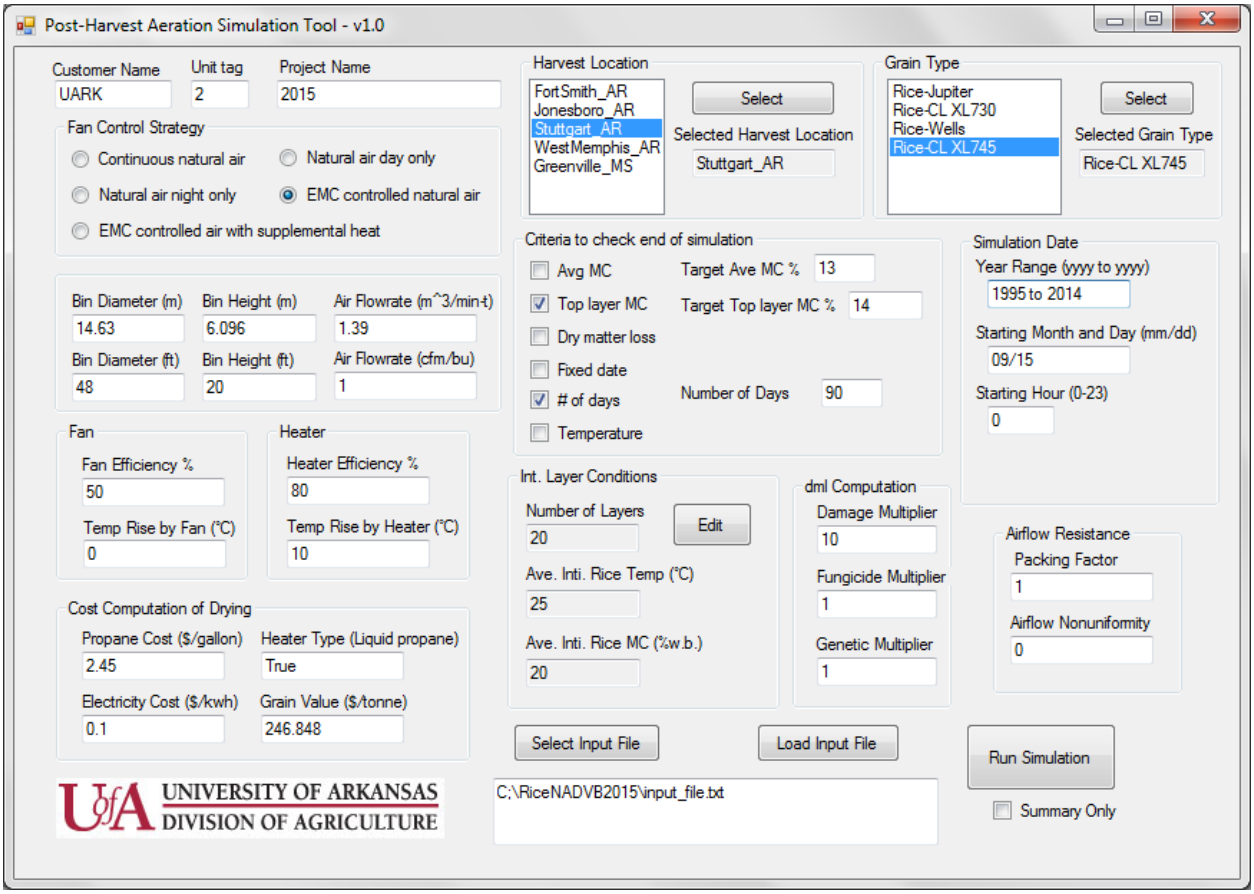

Figure 3.2. Post-Harvest Aeration Simulation Tool user interface

3.3 Simulations for model validation

Mathematical simulations of NA, in-bin drying of rice were performed. Simulation outputs included rough rice MC, temperature, and DML profiles for rough rice layers throughout drying period, and the average, maximum, and minimum MC and temperature of rough rice, average and maximum DML of rough rice, percent overdrying, drying duration, and fan and heater run durations.

Simulation results were compared with data obtained from field experiments, which were conducted in the 2014 rice drying period. Temperature and RH data from sensors installed in the bins, used in this study, were acquired, and the rough rice MCs were calculated based on

empirical relationships. For proprietary purposes, the empirical equation used by the sensor manufacturing company (OPI-Systems Inc., Calgary, Alberta, Canada) to calculate the rough rice MC is not documented. However, validation of results obtained from the sensors were performed. The model validation was split into two parts.

- Compare meter-measured rough rice MC (i.e. MC determined in the lab using the AM5200 grain moisture tester (Perten Instruments Inc., Hägersten, Sweden) calibrated according to oven-moisture method measurement of rough rice (Jindal & Siebenmorgen, 1987) with the field sensor-determined data of rough rice MC in two bins located at Burdette and Dermott, Arkansas [Figure 3.3 (bins A and B, respectively)].
- Compare field sensor-determined data of MC and temperature with the simulated MC and temperature of rough rice in two bins located at Dermott, Arkansas [Figure 3.3 (bins C and D)].

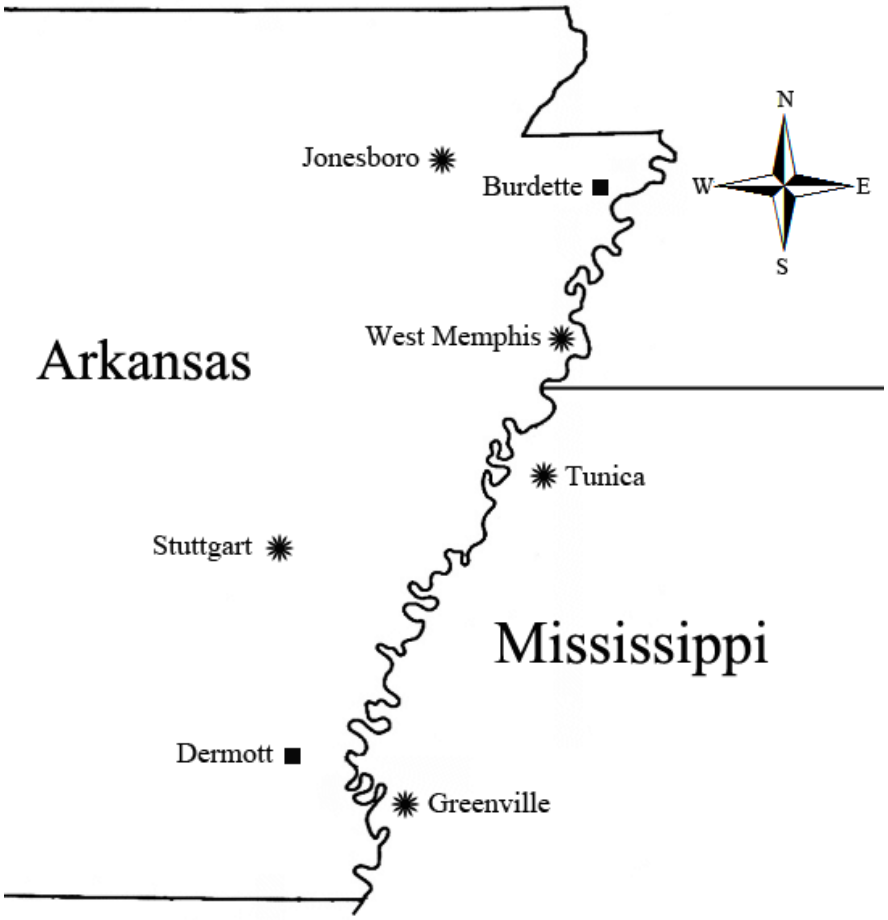

Figure 3.3. Rice-growing locations in the U.S. Mid-South. Squares (■) represent the bin locations used in validation study, and stars (✷) represent the bin locations used in the simulations of impacts of various drying strategies.

Rough rice was sampled 1.22 m (4 ft) beneath the center surface from bins A and B using a partitioned brass sampling probe (Seedburo Equipment Co., Des Plaines, Ill.). Sampling was performed every two weeks, thus: at 0, 2, 4, 6, 8, and 10 weeks or until the top grain layer reached safe storage MC of 14%. Each sample weighed about 600 g. The rough rice samples were immediately packed in sterile polyethylene bags and transferred under refrigerated conditions to the lab for immediate MC analysis using the grain moisture tester (AM 5200, Perten Instruments Inc., Hägersten, Sweden). The grain moisture tester was calibrated using the oven-moisture method of rough rice (Jindal & Siebenmorgen, 1987) . The meter-measured MCs

were compared with the rough rice MC calculated from data recorded by the sensors. The data from the sensors was provided by the grain bin management company (OPI-Systems Inc., Calgary, Alberta, Canada).

During the field experiments, there were some incidences, such as power outage, unplanned changes of fan control strategy settings, (e.g. manual override of the fan control strategy), or even movement of the rice in the bin. Accurate accounting for such incidences in simulations and validations was problematic, especially for bins A and B (table 3.2). However, a separate set of bins (C and D) which did not have the above incidences were selected for additional model simulation and validation. The meter-measured data of MC for bins C and D will not be presented in the results since the bin selection was after it was determined that drying progressed without interruption by the uncontrollable circumstances. Specifications of bins A, B, C, and D are listed in table 3.2. Temperature cables and temperature and humidity (TH) cables were suspended from the bin roof. The sensors were 1.22 m (4 ft) apart from each other on each cable.

Weather conditions at Greenville, Mississippi, including hourly temperature and RH, were used as in-let air conditions for the Dermott, Arkansas location (48 km apart and the closest weather station). Hourly temperature and RH data of Greenville, Mississippi were procured from accuweather.com (AccuWeather, Inc., State College, Pa.). The EMC-NA fan control strategy was used in both bins C and D, but with different target EMC ranges (table 3.2). For EMC-NA fan control strategy, fan operation was switched off in one of the two cases (1) when both the plenum air EMC and bottom layer rough rice MC were less than the set EMC low limit, or (2) when both the plenum air EMC and the bottom layer rough rice MC were greater than the set EMC high limit. In table 3.2, the simulation-start date and time were set to be at the time when

the bin filling was finished; the simulation-end date and time were when actual sensor readings were equal to or lower than the targeted EMC. The air flowrate in the bins were not measured but calculated.

Table 3.2. Configurations and drying strategies of bins A, B, C, and D.

	Bin A	Bin B	Bin C	Bin D
Bin Location	Burdette, Ark.	Dermott, Ark.	Dermott, Ark.	Dermott, Ark.
Sensor Locations	Center and side	Center and side	Center and side	Center and side
Bin Diameter	14.63 m (48 ft)	14.63 m (48 ft)	14.63 m (48 ft)	14.63 m (48 ft)
The Top-most Sensor Depth	Center: 7.32 m (24 ft) Side: 6.1 m (20 ft)	Center: 7.32 m (24 ft) Side: 6.1 m (20 ft)	Center: 7.32 m (24 ft) Side: 6.1 m (20 ft)	Center: 7.32 m (24 ft) Side: 6.1 m (20 ft)
Fan Configuration	40 HP 1750 RPM centrifugal fan; 2 fans in parallel	40 HP 1750 RPM centrifugal fan; 2 fans in parallel	30 HP 1750 RPM centrifugal fan; 2 fans in parallel	30 HP 1750 RPM centrifugal fan; 2 fans in parallel
[1]Fan Control Strategy	EMC-H	EMC-NA	EMC-NA	EMC-NA
Target EMC	12.5% (w.b.)	12.5% (w.b.)	12.5% (w.b.)	12.5% (w.b.)
Targeted EMC Range	N/A	14.5% - 10.5% (w.b.)	13.5% - 10.5% (w.b.)	14.5% - 10.5% (w.b.)
Issues for Simulation and Validation	Targeted EMC limits changed during the drying period	One fan was off during the first half of drying period	N/A	N/A
Simulation-start Date and Time	N/A	N/A	26 Sept. 2014 at 12:00 AM	03 Oct. 2014 at 4:00 AM
Simulation-end Date and Time	N/A	N/A	21 Oct. 2014 at 11:59 PM	27 Oct. 2014 at 11:59 PM
[2]Initial Rough Rice Temperature (°C)	N/A	N/A	Sensor6=20.44, Sensor5=20.39, Sensor4=21.11, Sensor3=21.61, Sensor2=21.56, Sensor1=22.83.	Sensor6=26.33, Sensor5=26.17, Sensor4=26.11, Sensor3=26.00, Sensor2=24.11, Sensor1=24.94.

[2]Initial Rough Rice Moisture Content (%.w.b.)	N/A	N/A	Sensor1=15.32, Sensor2=16.95, Sensor3=16.67, Sensor4=17.96, Sensor5=17.56, Sensor6=16.01.	Sensor1=14.74, Sensor2=16.84, Sensor3=16.38, Sensor4=18.69, Sensor5=19.58, Sensor6=19.53.
Plenum pressure	N/A	N/A	1673.03 Pa (6.71 in H_2O)	1637.07 Pa (6.57 in H_2O)

[1] EMC-H represents equilibrium moisture content controlled air with supplemental heat fan control strategy; EMC-NA represents equilibrium moisture content controlled natural air fan control strategy.
[2] Sensor1 represented the first (bottom) layer, and Sensor2 represented the second layer MC which was 1.22 m (4 ft) above the first layer. Therefore, Sensor6 was 7.32 m (24 ft) from the bottom of the bin.

To calculate air flowrate of two fans in parallel, the airflow resistance equation listed in ASABE Standard D272.3 (ASABE Standards, 2011) was used. The fan curve for a one fan system was provided by the fan manufacture (The GSI Group, Assumption, Ill.) (figure 3.5). The total air flowrate for a two-fan system was calculated by multiplying the total air flowrate of the one-fan system at a given work by two. The airflow resistance curve was calculated using equation (9), which took into account rice depth and a correction factor for the cleanness of the rice. The cross point between the airflow resistance curve and the two-fan curve determined the air flowrate when the two fans were arranged in parallel. For bins C and D, the top-most center sensor was located 7.32 m (24 ft) from the bottom, and the top-most side sensor was located 6.10 m (20 ft) from the bottom (figure 3.4). The side cable was installed 4.88 m (16 ft) from the center in a 14.64 m (48 ft) diameter bin. Bin coring (removal of grain at the bin center or core and returning it to the bin top) was implemented in bins C and D to improve uniformity of airflow (figure 3.4). The center rice height was 8.53 m (28 ft), and side height was 7.32 m (24 ft). For rough rice, the angle of repose of filling (γ) is 20 °, and the angle of repose of emptying (β) is 36 ° (Boac, Casada, Maghirang, & Harner III, 2010). The average heights of rice column in bins C and D were about 7.62 m (24 ft) based on the assumption that the rough rice layer above the sensors were 1.2 m (4 ft) thick (figure 3.4). The average height was calculated using the bin

volume divided by the horizontal cross-section area of the bin. The rice was assumed to contain medium level of foreign materials (correction factor C = 1.3). The cross point of two-fan curve and resistant curve indicated the total airflow was 765 m^3 min^{-1} (27,000 cfm). Both bins had air flowrate of 1.07 m^3 $min\text{-}t^{-1}$ (0.77 cfm bu^{-1}) (figure 3.5).

$$\frac{\Delta P}{L} = \frac{aQ^2}{\log_e(1+bQ)}C \tag{9}$$

where, ΔP – pressure drop (Pa); L – grain column depth (m); Q – airflow (m^3 $s\text{-}m^{-2}$); a and b are grain specific constants. For rough rice, a = 2.24×10^4 (Pa s^2 m^{-3}) and b = 13.2 (m^2s m^{-3}) when Q ϵ (0.0056, 0.152). The term C is the correction factor which depends on the cleanness of the rice (1 represents clean kernels only, and 1.5 represents rice with maximum amount of foreign materials).

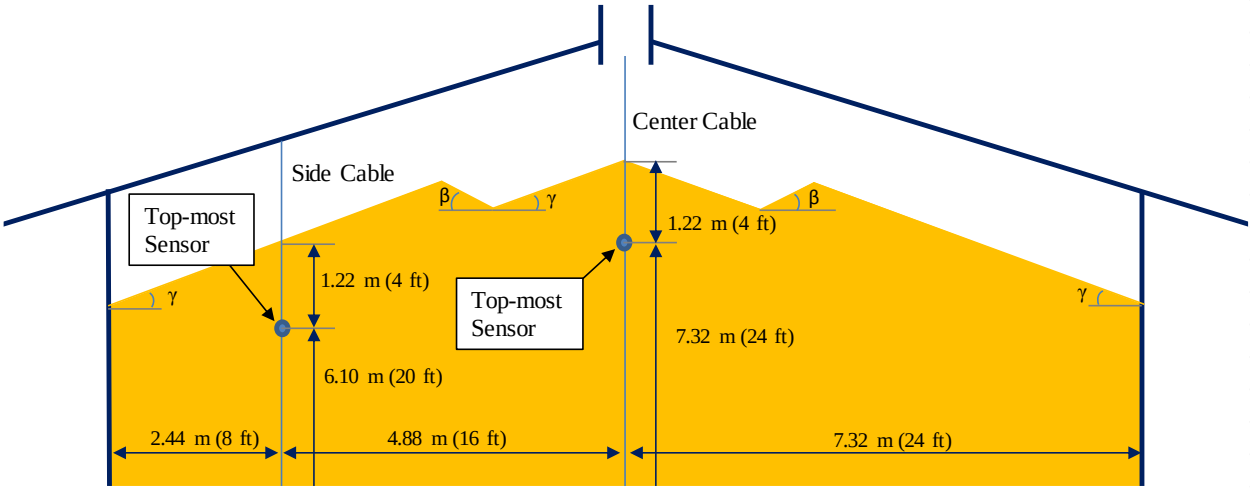

Figure 3.4. Schematic diagram of top layer rough rice in bins C and D. The bin radius is 7.32 m (24 ft), and the side cable was located 4.88 m (16 ft) from the center. The bins was cored. The top-most sensor of center cable was located 7.32 m (24 ft) from the bottom, and top-most sensor of side cable was located 6.10 m (20 ft) top from the bottom. The rough rice layer above the sensors was 1.22m (4 ft) thick. β represents angle of repose of emptying (for rough rice, β = 36 °), and γ represents angle of repose of filling (for rough rice, γ = 20 °).

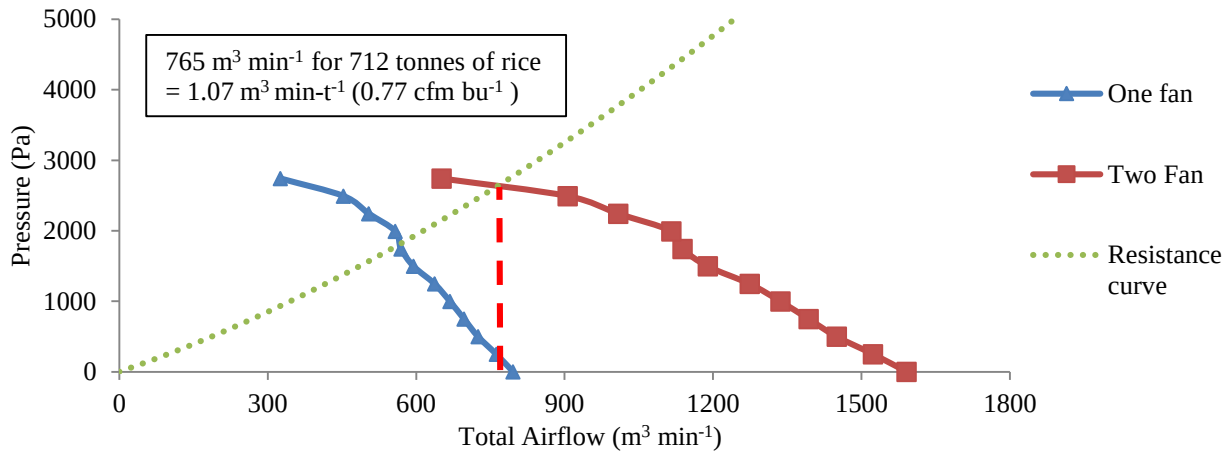

Figure 3.5. Resistance curve for rough rice and total airflow in a bin system with one fan and two fan arrangements.

3.4 Simulations to assess impact of in-bin rough rice drying strategies

Simulations were perform to evaluate implications of three fan control strategies comprising continuous NA (CNA), EMC-NA, and running the fan at set windows of drying air EMC-controlled air with supplemental heat (EMC-H). For each fan control strategy, rough rice at four IMC levels (16%, 18%, 20% and 22%) were dried at four air flowrates of 0.69, 1.39, 2.08, and 2.77 m^3 $min\text{-}t^{-1}$ and drying-start dates of 15 August, 15 September, and 15 October. The simulations were performed using weather from representative rice-growing locations in the Mid-southern region of the U.S. (Jonesboro, West Memphis, and Stuttgart, Arkansas, and Greenville and Tunica, Mississippi (figure 3.3)). Twenty-year weather data (1995 to 2014) of hourly ambient air temperature and RH were procured from accuweather.com (AccuWeather, Inc., State College, Pa.) for simulation purposes.

For EMC-H fan control strategy, fan operation was switched off when both the plenum air EMC and bottom-layer rough rice MC were less than the set EMC low limit, or the heater would be switched on when both the plenum air EMC and the bottom layer rough rice MC were

greater than the set EMC high limit. For both EMC-H and EMC-NA fan control strategies, the set EMC high limit was one percentage point MC greater than the targeted EMC (equation 10), and a dynamic EMC low limit was used (equation 11). The fan-operation window narrowed as the rough rice MC approached the targeted EMC:

$$EMC_{high\ limit} = EMC_{targeted} + 1 \tag{10}$$

$$EMC_{low\ limit} = EMC_{targeted} - \frac{\left(MC_{average} - MC_{bottom}\right)}{2} \tag{11}$$

where, $EMC_{high\ limit}$ – the highest limit of the targeted EMC in percentage wet basis; $EMC_{targeted}$ – the targeted EMC in percentage wet basis; $EMC_{low\ limit}$ – the lowest limit of the targeted EMC in percentage wet basis; MC_{bottom} – bottom layer MC in percentage wet basis; $MC_{average}$ – average MC in percentage wet basis.

An rough rice column was divided into 20 thin layers for simulation purposes. The depth of rough rice in the bin was assumed to be 6.10 m (20 ft) which implied that each layer of rough rice had a thickness of 0.31 m. For a bin with diameter of 14.63 m (48 ft) containing 1,205 m^3 (29,082 bu) of rice, the air velocities inside the bins were determined to be 0.04, 0.08, 0.12, and 0.16 m s^{-1} for 0.69, 1.39, 2.08, and 2.77 m^3 min-t^{-1} air flowrates, respectively, which were relatively slow. Thus, it was assumed that the drying air and the rough rice within each layer reached temperature and moisture content equilibria air to grain within a specified time step (10 min). Each simulation was ran for 90 days or stopped earlier if the top layer of rough rice dried to MC of 14%. Each simulation provided outputs of the total drying duration and final rough rice maximum DML, average rice MC, maximum MC, and minimum MC. The rate of overdrying was determined by calculating the percentage of the number of rice layers in the grain bin that would dry to MC below 12% out of 20 layers. Table 3.3 illustrates the simulation design carried out for this research.

Table 3.3. Simulation design for assessment of implications of natural air, in-bin drying strategies for rough rice in the U.S Mid-south.

Fan Control Strategy*	Air Flowrate (m^3 $min\text{-}t^{-1}$)	Initial Moisture Content (%, wet basis)	Drying-start Date	Simulation Year	Drying Location
CNA	0.69 (0.5 cfm bu^{-1})	16	15 Aug.	1995 to 2014	Jonesboro, Ark.
EMC-NA	1.39 (1 cfm bu^{-1})	18	15 Sept.		West Memphis, Ark.
EMC-H	2.08 (1.5 cfm bu^{-1})	20	15 Oct.		Tunica, Miss.
	2.77 (2 cfm bu^{-1})	22			Stuttgart, Ark.
					Greenville, Miss.

***** CNA – Continuous natural air fan control strategy; EMC-NA – Equilibrium moisture content controlled natural air fan control strategy; EMC-H – Equilibrium moisture content controlled air with supplemental heat fan control strategy.

3.4 Statistical analysis

Results of rough rice MC during desorption and adsorption versus temperature and water activity (RH in decimal) were analyzed using nonlinear regression in JMP (JMP 12.0.0, SAS Institute, Inc., Cary, N.C.) to estimate the empirical constants (A, B, and C) of the four EMC models in table 1.1. Root mean square errors (RMSEs) between the predicted and meter-measured EMC results were calculated and compared. The RMSE was calculated by using equation 12. The main effects of all variables on EMC and statistical parameters were determined using ANOVA (JMP 12.0.0, SAS Institute, Inc., Cary, N.C.), and statistical significance (α) was set to 0.05.

Excel software (Microsoft Office 2013, Microsoft Corp., Redmond, Wash.) was used to calculate the RMSE, Nash-Sutcliffe efficiency (NSE), and Percent bias (PBIAS) to evaluate the

relationships among meter-measured sample MCs, the sensor-determined MCs, and MCs obtained from simulation output. The NSE defines the relative magnitude of the residual variance compared to the measured data variance (Nash & Sutcliffe, 1970). The NSE value ranges between -∞ and 1; value of 1 represents a perfect match of model to observed data. The NSE was calculated by using equation 13. NSE value equal to zero indicates that the model predictions are as accurate as the mean of the observed data. The PBIAS measures the average tendency of the simulated data to be larger or smaller than their observed counterparts (Gupta, Sorooshian, & Yapo, 1999). The PBIAS value is expressed in percentage and ranges between -∞ and +∞ and was calculated by using equation 14.

$$\text{RMSE} = \sqrt{\frac{\sum_{i=1}^{N}\left(Y_i^{obs} - Y_i^{sim}\right)^2}{N}} \tag{12}$$

$$\text{NSE} = 1 - \frac{\sum_{i=1}^{N}\left(Y_i^{obs} - Y_i^{sim}\right)^2}{\sum_{i=1}^{N}\left(Y_i^{obs} - Y_i^{mean}\right)^2} \tag{13}$$

$$\text{PBIAS} = \frac{\sum_{i=1}^{N}\left(Y_i^{obs} - Y_i^{sim}\right) * 100}{\sum_{i=1}^{N}(Y_i^{obs})} \tag{14}$$

where, Y_i^{obs} – observed or measured rough rice MCs; Y_i^{sim} – simulated or sensor predicted rough rice MCs; and Y_i^{mean} – the mean of observed or measured rough rice MCs; and N – the number of data points.

4. RESULTS AND DISCUSSION

4.1 Sorption isotherms estimation

Average EMCs of rough rice CL XL745 under various temperatures (15 ℃, 25 ℃, and 35 ℃) and RHs (10%, 30%, 50%, 70%, and 90%) are listed in figure 4.1 and table 4.1. Table 4.1 shows that rough rice EMC significantly increased when air temperature decreased, or air RH increased in both adsorption or desorption isotherms. Comparing the adsorption EMC and desorption EMC for all the three temperatures at 30%, 50%, and 70% RHs indicated that the average desorption EMC was 2.14 percentage point MC higher than average adsorption EMC. For 10% or 90% RHs, the average adsorption EMC was very similar (less than half a percentage point MC) to the average desorption EMC for each temperature (figure 4.1). Missing data at 15 ℃ and 90% RH condition was due to the limitation of the VSA to obtain data at that condition.

For each moisture sorption model listed in table 1.1, nonlinear regression analysis was used to determine empirical constants A, B, and C of adsorption and desorption isotherms for the ranges of temperature and RH studied. The empirical constants, generated using the data listed in table 4.1, are listed in table 4.2 alongside the RMSEs between the predicted and the meter-measured EMC results. The new empirical constants are also compared with the constants listed in ASABE Standard D245.6 (2012) in table 4.2. Modified Chung-Pfost equation was the best fit for the desorption isotherms with the lowest RMSE (0.54% MC in dry basis), and Modified Halsey equation was the best fit for the adsorption isotherm with the lowest RMSE (0.91% MC in dry basis).

The sum of RMSEs (SRMSE) of modified Chung-Post equation for the desorption isotherms and modified Halsey equation for the adsorption isotherms resulted in the smallest

SRMSE (0.54% + 0.91% = 1.43% MC in dry basis); however, it seemed not theoretically accurate to use two sets of equations to simulate NA drying of rough rice in some temperature and RH conditions. For instance, figure 4.2 indicated that the predicted adsorption EMC of rough rice would be greater than predicted desorption EMC when air temperature and RH are at 30 ℃ and 95%, respectively. Since desorption EMCs are always higher than or equal to the adsorption EMCs (Brooker, Bakker-Arkema, & Hall, 1992; Choi et al., 2010), the combination of modified Chung-Post and modified Halsey equations would generate calculation errors at the high RH conditions, and this error would carry over in the finite difference model and affect the accuracy of predicted results. Therefore, the combination of modified Chung-Post and modified Halsey equations was not used in the simulation to predict the EMC. Figure 4.3 illustrates the desorption and adsorption EMCs at temperature of 10 ℃ to 40 ℃ and RH of 1% to 99% as predicted by the modified Chung-Post equation with the desorption and adsorption constants listed in table 4.2. The results showed that EMC decreased as temperature increased, and desorption EMCs were always higher than or equal to the adsorption EMCs. In figure 4.3, the desorption and adsorption EMCs were also compared with EMCs of long-grain rough rice (CL XL730) predicted by the modified Chung-Post equation with the constants listed in study of Ondier et al. (2011) for the same air condition.

The SRMSE for each equation gives an estimation of the overall difference between the equations. The SRMSE of Modified Halsey equation was 0.09 percentage point MC (dry basis) lower than the SRMSE of Modified Chung-Pfost equation (table 4.2). Previous studies had shown that Modified Chung-Pfost equation was the best for describing EMC of rough rice for different temperature and RH ranges (Sun, 1999; Iguaz & Versada, 2007; Ondier et al., 2011). Since only one equation could be used in the simulation model, the Modified Chung-Pfost

equation was selected for use in the simulation to describe desorption and adsorption EMCs of long-grain rough rice at various air conditions.

Table 4.1. Equilibrium moisture contents of long-grain hybrid rice cultivar CL XL745 at temperatures ranging from 15 ℃ to 35 ℃ and relative humidities ranging from 10% to 90% in desorption and adsorption conditions. For each sorption type and relative humidity combination, values within individual rows followed by the same lowercase letter are not significantly different. For each sorption type and temperature combination, values across individual columns followed by the same uppercase letter are not significantly different.

Relative Humidity (%)	Temperature (℃)					
	15	25	35	15	25	35
	Adsorption Equilibrium Moisture Content (%w.b.)			Desorption Equilibrium Moisture Content (%w.b.)		
10	11.9 a B	10.0 ab D	9.0 b D	12.4 a' D'	9.9 b' E'	9.1 b' E'
30	12.3 a B	10.5 ab D	9.5 b D	13.9 a' C'	12.3 b' D'	10.8 c' D'
50	13.3 a B	12.5 a C	12.0 a C	16.3 a' B'	15.0 ab' C'	14.0 b' C'
70	16.1 a A	15.8 a B	15.6 a B	18.8 a' A'	18.5 a' B'	17.3 a' B'
90		22.6 a A	22.3 a A		22.6 a' A'	22.3 a' A'

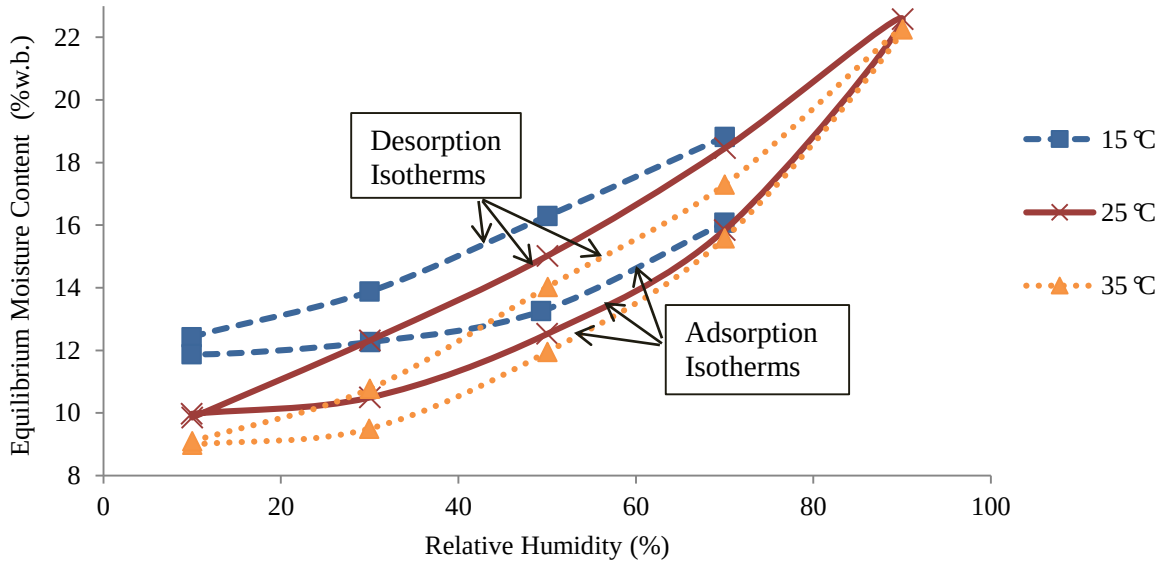

Figure 4.1. Equilibrium moisture contents of long-grain hybrid rice cultivar CL XL745 at temperatures ranging from 15 ℃ to 35 ℃ and relative humidities ranging from 10% to 90% in desorption and adsorption conditions.

Table 4.2. Constants, root mean square errors (RMSEs), and sums of RMSE (SRMSEs) of Modified Chung-Pfost, Modified Halsey, Modified Henderson, and Modified Oswin equations used for predicting desorption and adsorption isotherms of long-grain rough rice

Model	Sorption Type	Source	Model Constants			RMSE (%MC d.b.)	SRMSE (%MC d.b.)
			A	B	C		
Modified Chung-Pfost	Desorption	Experiment*	861.4998	0.2382	9.6002	0.54	1.86
		ASABE†	579.9479	0.1894	52.1784		
		ASABE‡	412.02	0.17528	39.016		
	Adsorption	Experiment*	1086.5411	0.2454	29.8549	1.32	
		ASABE†	590.3090	0.1936	55.2229		
Modified Halsey	Desorption	Experiment*	10.9302	-0.0320	3.9053	0.86	1.77
		ASABE†	8.1726	-0.006112	3.3578		
	Adsorption	Experiment*	9.0526	-0.0183	3.4783	0.91	
		ASABE†	8.3821	-0.01029	3.3874		
Modified Henderson	Desorption	Experiment*	8.0518×10^{-7}	3.5691	21.4187	2.34	4.34
		ASABE†	2.9747×10^{-5}	2.1177	79.1993		
		ASABE‡	4.1276×10^{-5}	2.1191	49.828		
	Adsorption	Experiment*	8.9734×10^{-7}	3.3119	93.1951	2.00	
		ASABE†	3.3900×10^{-5}	2.1226	73.0724		
Modified Oswin	Desorption	Experiment*	17.9920	-0.1104	5.2319	0.79	2.11
		ASABE†	13.1323	-0.02873	3.9156		
		ASABE‡	14.431	-0.07886	3.137		
	Adsorption	Experiment*	15.0560	-0.0560	4.7226	1.32	
		ASABE†	13.4692	-0.04410	3.9542		

*Constants generated using JMP 12.0.0 based on the experimental result of this study for predicting desorption and adsorption isotherms of long-grain hybrid rough rice (cv. CL XL745).
†Constants generated using JMP 12.0.0 based on the equilibrium moisture content data listed in ASABE Standard D245.6 (2012) for long-grain rough rice (cv. Inga) in desorption and adsorption conditions.
‡Constants listed in ASABE Standard D245.6 (2012) for long-grain rough rice.

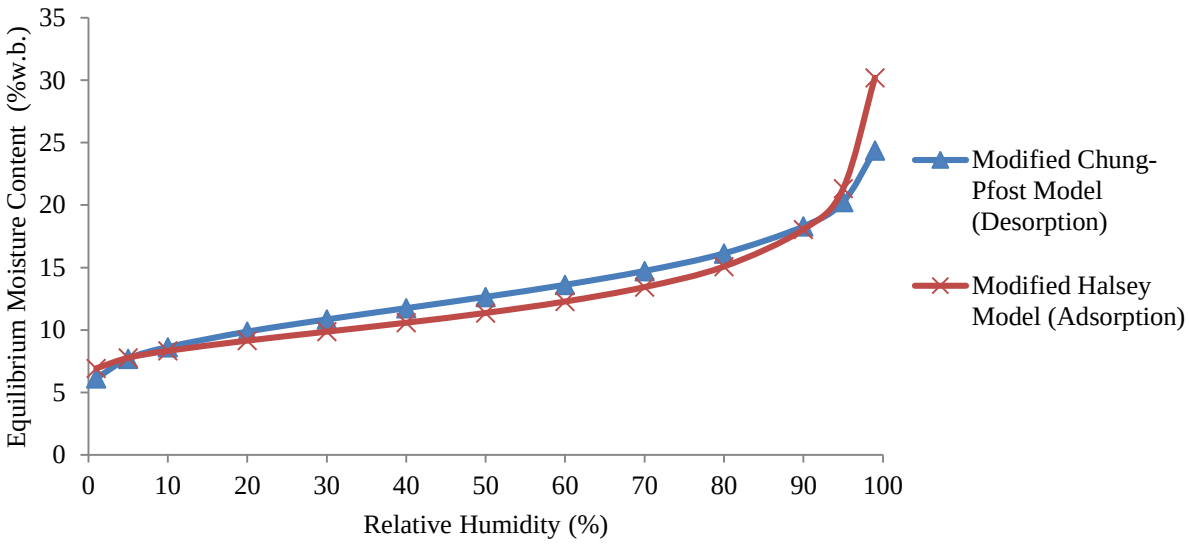

Figure 4.2. Equilibrium moisture content isotherms (% wet basis) predicted by the modified Chung-Pfost equation in desorption condition (—▲—) and modified Halsey equation in adsorption condition (—×—) at temperature of 30 ℃. Model constants A, B, and C of modified Chung-Pfost equation are 861.4998, 9.6002, and 0.2382. Model constants A, B, and C of modified Halsey equation are 9.0526, -0.0183, and 3.4783.

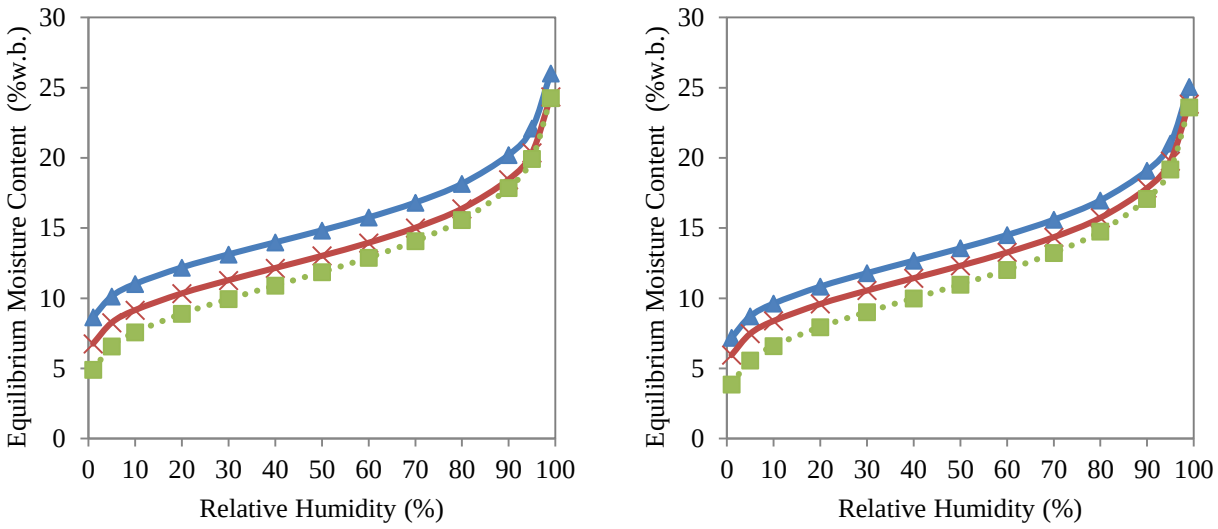

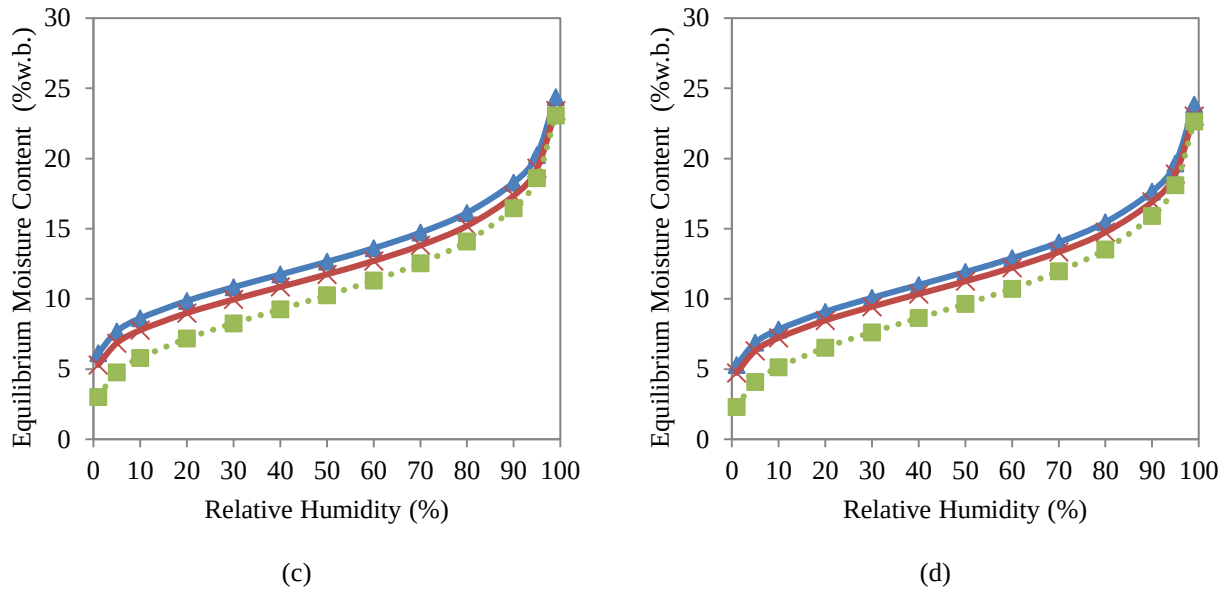

Figure 4.3. Equilibrium moisture content isotherms (% wet basis) of long grain rough rice predicted by the modified Chung-Pfost equation from present study (desorption (—▲—) and adsorption (—✕—) conditions) compared to data from Ondier et al. (2011) (···■···) at temperature of (a) 10 ℃, (b) 20 ℃, (c) 30 ℃, and (d) 40 ℃. For present study, model constants A, B, C are 861.4998, 9.6002, 0.2382 and 1086.5411, 29.8549, 0.2454 for desorption and adsorption conditions, respectively. For Ondier et al. (2011) study, model constants A, B, C are 501.7992, 23.6330, and 0.2279.

4.2 Simulations for model validation

4.2.1 Meter-measured data vs. sensor-determined data

Table 4.3 shows the rough rice MC which was calculated from the temperature and RH data corresponding to the top-most sensor on the center cable. The calculated rough rice MCs were compared with meter-measured MC of rough rice samples at the top-most sensor location of the center cable in bins A and B. RMSE values showed that the meter-measured MC data were 1.48 percentage point MC and 0.73 percentage point MC lower than the MC values calculated from temperature and RH data of in-bin sensors in bins A and B, respectively. PBIAS values indicated that the rough rice MC values determined using the sensor data over-predicted the meter-measured rough rice MC data by 7.60% and 4.54% for rice in bin A and B,

respectively. The variation between the meter-measured and sensor-determined MCs could be related to (1) variation of sampling points relative to the sensor position, (2) the accuracy of prediction of temperature and RH by the sensors, and (3) accuracy of the equation used to calculate the rough rice MC from the temperature and RH data. In this study, rice samples were consistently taken within 0.61 m (2 ft) radius from the sensor. It was assumed that within that radius, the rough rice MC variability was negligible based on recommendations provided by sensor manufacturing company (OPI-Systems Inc., Calgary, Alberta, Canada) for spacing the sensors in a 14.6 m (48 ft) diameter bin. In general, sensor-determined rough rice MC data followed a similar trends as meter-measured data during the drying.

Table 4.3. Sensor-determined moisture content (MC) and meter-measured MC data for rough rice in bins A and B; comparison of root mean square errors (RMSEs) and percent biases (PBIASs). Rice in the bin was sampled 1.22 m (4 ft) below the top-most layer surface at the center.

Bin location	Sampling Date	In-bin Sensor-determined MC data (%w.b.)	Meter-measured MC (%w.b.)	RMSE (%w.b.)	PBIAS (%)
Bin A (Dermott, Ark.)	12/10/2014	20.33	19.22	1.48	7.60
	26/10/2014	20.62	19.22		
	9/11/2014	19.64	17.35		
	21/11/2014	14.76	14.24		
Bin B (Burdette, Ark.)	13/9/2014	16.33	15.53	0.73	4.54
	27/9/2014	16.36	16.13		
	11/10/2014	13.83	12.72		
	25/10/2014	13.07	12.62		

4.2.2 Sensor-determined data vs. simulation results

Since rough rice located at the center top of the bin normally suffers the greatest quality impact during NA, in-bin drying, simulation and validation studies focused on the center rough

rice temperature and MC profiles. Figures 4.4 (a) and (b) show the simulated rough rice MC profiles (dashed lines) and the cable sensor-determined rough rice MC profiles (solid lines) in bins C and D, respectively. In both bins C and D, rough rice drying progressed from the bottom to the top to reach 14% MC or below in about 20 days. In figures 4.4 (a) and (b), the simulated rough rice MC profiles of the first five layers were similar to those of sensor-determined data. Fluctuations observed in results of figures 4.4 (a) and (b) are attributed to higher temperature and lower RH of air during the day compared to lower temperature and higher RH of air at night.

Figures 4.5 (a) and (b) illustrate the simulated rough rice temperature profiles (dashed lines) and the center cable sensor-recorded temperature profiles (solid lines) in bins C and D, respectively. As the air moved from the bottom to the top, the air temperature decreased due to evaporative cooling. Consequently, S1 (representing sensor 1, bottom-most sensor) recorded the highest temperature, and S6 (representing sensor 6, top-most sensor) recorded the lowest temperature for most of the drying duration (figure 4.5). Figures 4.5 (a) and (b) indicate that the rough rice temperature profiles determined using the sensors had lower daily temperature fluctuations than the temperature profiles from simulations. The reason could be due to the fact that in modeling of the rice drying, heat conduction and convection between the outside environment and the bin were assumed negligible.

For EMC-NA fan control strategy, if both the bottom layer rough rice MC and the air EMC are greater than set EMC limit, the fan operation will be stopped to avoid rewetting. Therefore, in figures 4.4 and 4.5, sections of the simulated rough rice MC and temperature profiles with horizontal straight lines (highlighted with boxes) indicated that the fans were turned off around 12 October. The increase in temperature and MC would be attributed to rough rice, bacteria, and mold respirations. The breakdown of rice carbohydrate produced heat, CO_2, and

water. Typically, rough rice with higher MC has a higher respiration rate. Comparing the rough rice MC and temperature increments between different layers in both bins around 12 October, it was noted that the upper layer of rough rice with the highest MC had the highest MC and temperature increments, and the lower layer of rough rice with the lowest MC had the lowest or no MC and temperature increments (figures 4.4 and 4.5). Higher respiration rate along with increasing temperature and MC also imply higher DML of the rough rice (equation 8). It is also reasonable that after the fan operation was stopped, the sensor-determined rough rice MC and temperature slowly increased due to the air and the rough rice having considerably longer time to reach true equilibrium.

Statistical comparisons of sensor-determined and simulated MC data of rough rice in bins C and D are listed in table 4.4 (a). The RMSEs of MC of rough rice in all layers for both bins were lower than or equal to 0.70% MC, except for the RMSE of the 6th layer of rice in bin C which was 1.07% MC. The NSE values indicated that except for the 6th layer of rice in bin C and 1st layer of rice in bin D (NSEs = 0.42 and -0.33, respectively), the simulated results of rough rice MC profiles of the other ten layers in both bins predicted well the sensor-determined rough rice MC data (NSEs > 0.45). PBIAS values indicated that simulated results of the rough rice MC profile of the 6th layer of rice in bin C overestimated the sensor-determined rough rice MC profile by 5.76%, and the rest of the eleven layers in both bins had PBIAS values between -3.53% and 3.22%. The faster drying rate of top layer rice in bin C could be due to nonuniform airflow in the grain mass. Uniform airflow throughout the grain mass could be restricted by materials other than grain (MOGs), such as fines and empty kernels. Comparing tables 4.3 and 4.4 (a), all PBIAS and RMSE values of simulated rough rice MC profiles versus sensor-determined rough rice MC profiles were less than the lowest PBIAS and RMSE values of sensor-

determined rough rice MC data versus meter-measured rough rice MC data, respectively, except the RMSE of the 6th layer of bin C. The statistical parameters indicated that overall rough rice MC prediction was accurate (table 4.4 (a)).

Statistical comparisons of sensor-recorded and simulated rough rice temperature data for bins C and D are listed in table 4.4 (b). The RMSEs were between 1.47°C and 2.28°C, and the NSEs were equal to or greater than 0.45. Similar to the results of MC comparison in bin C, the 6th layer of rice had the largest (in negative) PBIAS value which indicated that the simulated rough rice temperature profile underestimated the sensor-recorded rough rice temperature profile by 3.07%. The rest of rough rice layers in bin C had PBIAS values between -1.46% and 1.78%. The PBIAS values of results from bin D showed that all the simulated rough rice temperature profiles underestimated the sensor-recorded rough rice temperature profiles by -3.54% to -2.07% in bin D. So, the rough rice temperature prediction in bin D was precise but not accurate. Based on statistical analysis listed in table 4.4 (b), the rough rice temperature prediction followed a similar trend as sensor-recorded rough rice temperature data. In table 4.4 (b), RMSE values of the 1st rough rice layer of bin D showed it that had about 10% (2.28°C × (23°C)$^{-1}$ × 100%) temperature difference from the sensor-recorded data, but PBIAS of same layer showed that the prediction error was just -3.54% which was much smaller than the difference calculated based on RMSE. The reason was that RMSE took into account all the differences ($\Sigma(Y^{obs}-Y^{sim})^2$), but the overestimation and underestimation values cancelled each other out in the PBIAS calculation ($\Sigma(Y^{obs}-Y^{sim})$). Therefore, it is important to determine the NSE value to point out if the two sets of data match each other based on the variance ($\Sigma(Y^{obs}-Y^{sim})^2/(\Sigma(Y^{obs}-Y^{mean})^2$).

Mean RMSE, NSE, and absolute PBIAS values of bins C and D are listed in table 4.4. For bins C and D, the mean RMSEs of rough rice MC are 0.54±0.29% MC and 0.57±0.10% MC,

respectively, the mean NSEs of rough rice MC are 0.79±0.23 and 0.68±0.50, respectively, and mean absolute PBIASs of rough rice MC are 2.23±2.00% and 2.37±0.97%, respectively (table 4.4 (a)). All mean RMSE, NSE, and absolute PBIAS values of rough rice MC between bins C and D were not significantly different ($\alpha = 0.05$). The mean RMSE, NSE, and absolute PBIAS values of rough rice MC indicated that the simulation accurately predicted rough rice MC profile. However, the mean RMSE and the mean absolute PBIAS of rough rice temperature in bins C (1.58±0.11°C and 1.11±1.21%, respectively) were significantly smaller than the mean RMSE and the mean absolute PBIAS of rough rice temperature in bin D (1.91±0.21°C and 2.96±0.69%, respectively). Also, the determined mean NSE of rough rice temperature in bin C (0.83±0.03) was significantly higher than that in bin D (0.49±0.04) ($\alpha = 0.05$). The statistical analysis indicated that the rough rice temperature profile predictions for bin C were more accurate than the temperature profile predictions for bin D. The variations between the results from the simulation and sensor-determined profiles could be due to the following reasons: (1) the EMC prediction difference. Under the same temperature and RH environment, the hysteresis was 2.14 percentage point MC (figure 4.1). Therefore, if the EMC calculation does not consider adsorption and desorption effects, the error on rough rice MC profile can be up to 2.14 percentage point MC under the same air condition. However, this could not be readily verified because the equation for predicting the EMC at the field was not disclosed to the researches due to proprietary reasons. (2) Sensing errors. As discussed in section 4.2.1, the RMSE between sensor-determined rough rice MC and meter-measured rough rice MC data were as large as 1.48 percentage point MC (table 4.3). (3) Weather condition difference. Weather plays a significant role in NA, in-bin drying. Since weather station, located at Greenville, Mississippi, was about 48

km (30 miles) from the location of the bins, the slight differences in weather condition between the two locations could lead to different drying patterns.

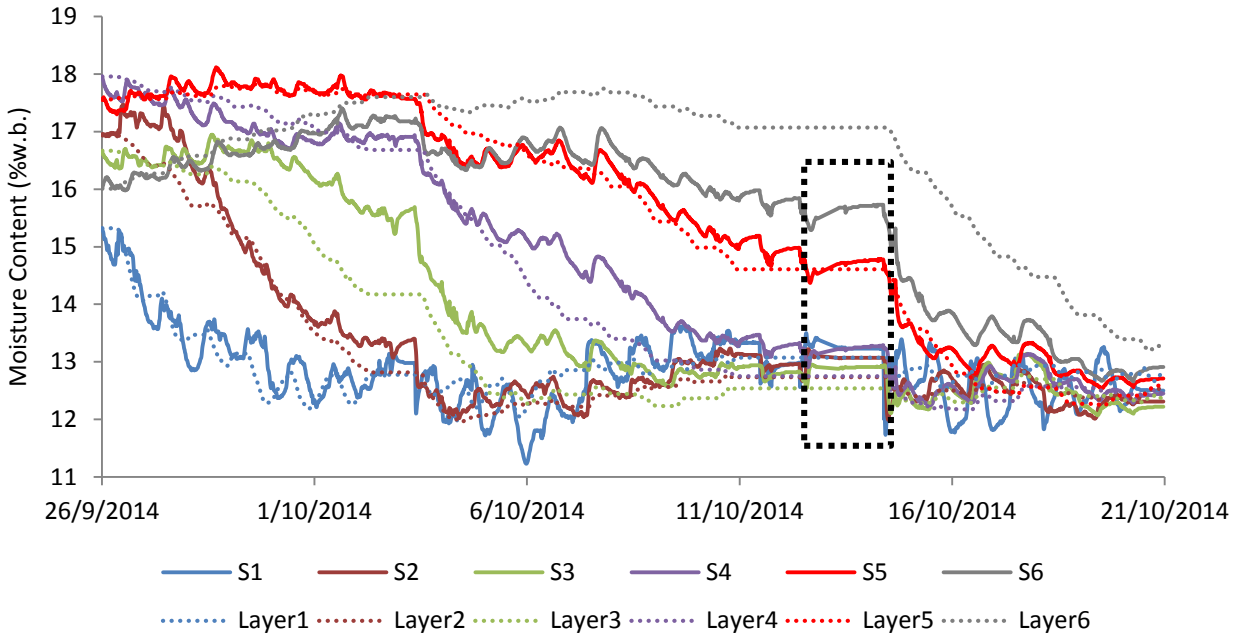

(a)

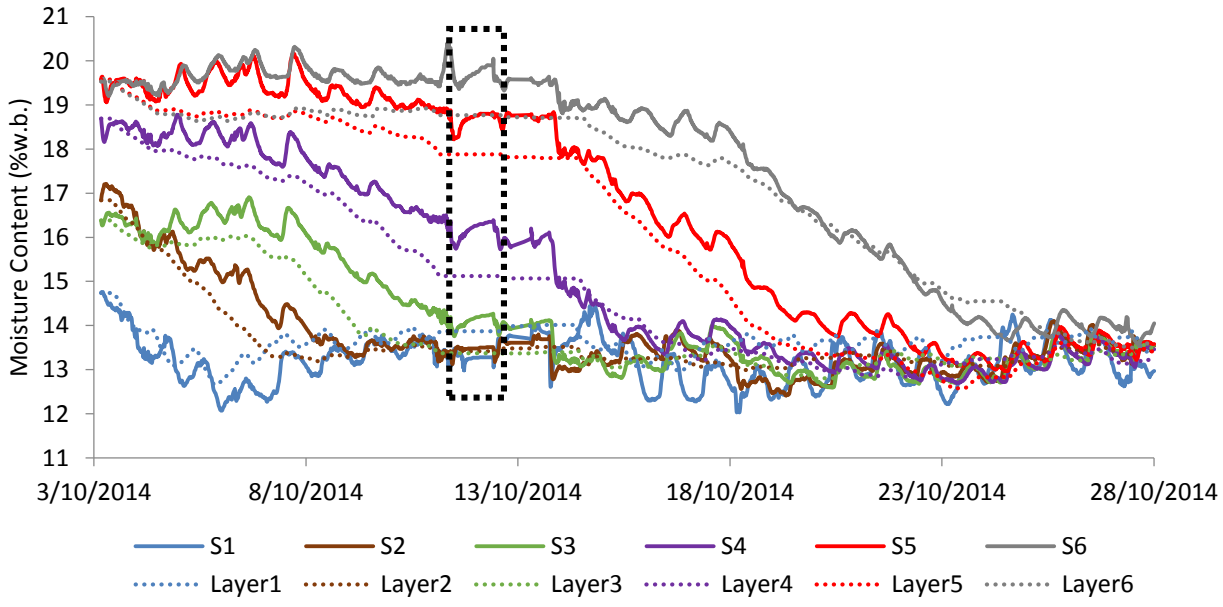

(b)

Figure 4.4. Comparison of moisture content (MC) determined using in-bin, center cable sensor data and simulations. Solid lines represent the in-bin cable sensor-determined data (S1-6), and the dashed lines represent the simulation results (Layer1-6). Layer1 and S1 represent the first (bottom-most) layer MC, and Layer2 and S2 represent the second layer MC. The sensors were 1.22 m (4 ft) apart; therefore, Layer6 and S6 are 7.32 m (24 ft) from the perforated screen floor. (a) bin C; (b) bin D.

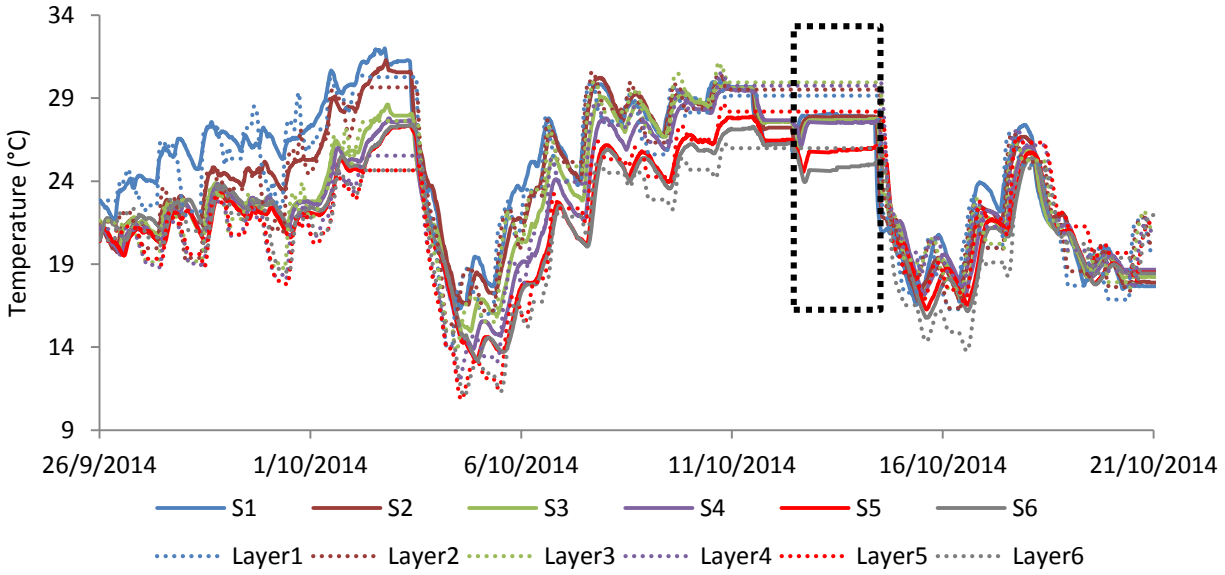

(a)

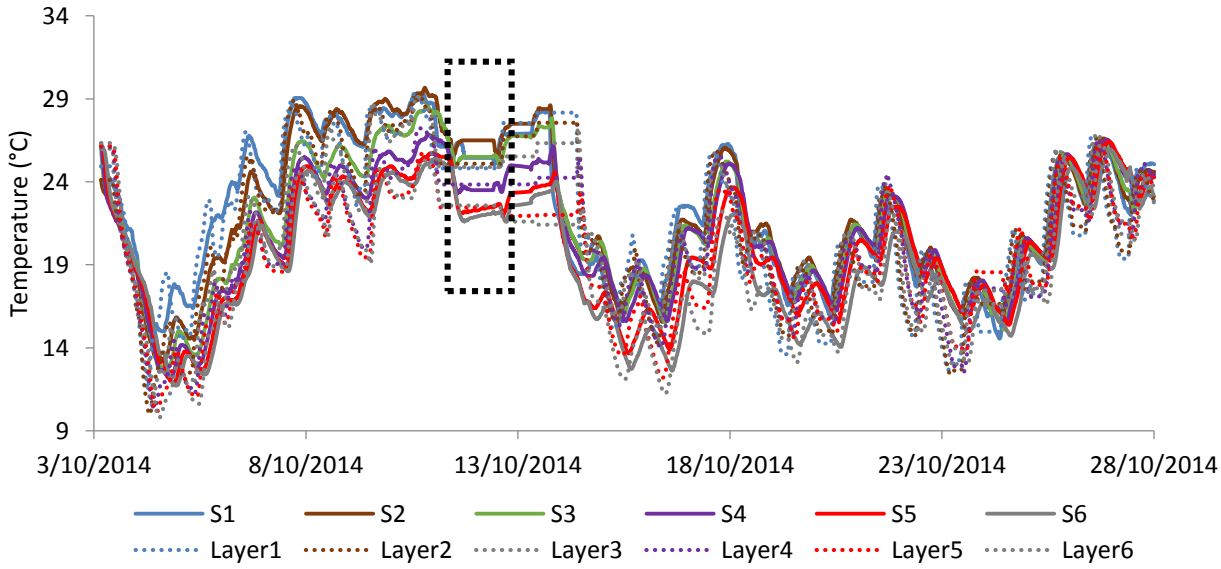

(b)

Figure 4.5. Comparison of in-bin, center cable sensor-recorded temperature and simulated rough rice temperature results. Solid lines represent the in-bin cable sensor readings (S1-6), and the dashed lines represent the simulation results (Layer1-6). (a) bin C; (b) bin D.

Table 4.4. Statistical parameters (Root mean square errors (RMSEs), Nash-Sutcliffe efficiencies (NSEs) and percent biases (PBIASs)) used to evaluate model performance for bins C and D. (a) comparison of moisture content calculated from sensor data of temperature and relative humidity and simulation, (b) comparison of temperature recorded by sensor and determined by simulations.

(a) Moisture Content Comparison

Bin C							
Layer	1	2	3	4	5	6	Mean
RMSE (% w.b. MC)	0.41	0.32	0.64	0.48	0.30	1.07	0.54 ±0.29*
NSE	0.60	0.95	0.85	0.94	0.97	0.42	0.79 ±0.23*
PBIAS (%)	0.46	-1.43	-3.31	-1.66	-0.73	5.76	2.23 ±2.00†
Bin D							
Layer	1	2	3	4	5	6	Mean
RMSE (% w.b. MC)	0.60	0.41	0.53	0.53	0.67	0.67	0.57 ±0.10*
NSE	-0.33	0.83	0.83	0.93	0.93	0.91	0.68 ±0.50*
PBIAS (%)	3.22	-0.87	-1.98	-1.99	-3.53	-2.65	2.37 ±0.97†

*Number represents one standard deviation from the mean. Mean = $\sum_{i=1}^{N}(Y_i)/N$

†Number represents one standard deviation from the mean absolute PBIAS. Mean absolute PBIAS = $\sum_{i=1}^{N}(|Y_i|)/N$

(b) Temperature Comparison

Bin C							
Layer	1	2	3	4	5	6	Mean
RMSE (°C)	1.77	1.47	1.55	1.60	1.62	1.47	1.58 ±0.11*
NSE	0.81	0.87	0.85	0.83	0.80	0.82	0.83 ±0.03*
PBIAS (%)	-1.46	0.06	1.78	0.12	0.17	-3.07	1.11 ±1.21†
Bin D							
Layer	1	2	3	4	5	6	Mean
RMSE (°C)	2.28	2.04	1.83	1.82	1.82	1.69	1.91 ±0.21*
NSE	0.56	0.48	0.46	0.50	0.50	0.45	0.49 ±0.04*
PBIAS (%)	-3.54	-3.96	-2.48	-2.85	-2.83	-2.07	2.96 ±0.69†

*Number represents one standard deviation from the mean. Mean = $\sum_{i=1}^{N}(Y_i)/N$

†Number represents one standard deviation from the mean absolute PBIAS. Mean absolute PBIAS = $\sum_{i=1}^{N}(|Y_i|)/N$

4.3 Simulations to assess impact of in-bin rough rice drying strategies

The implications of using fan control strategies (CNA, EMC-NA, and EMC-H) on duration of drying and maximum DML for rough rice at IMCs ranging from 16% to 22%, drying-start dates of 15 August, 15 September, and 15 October, air flowrates ranging from 0.69 to 2.77 m^3 $min\text{-}t^{-1}$ (0.5 to 2.0 cfm bu^{-1}) are shown in figures 4.6 and 4.7, respectively. Each error bar was constructed using 1 standard deviation from the mean. For each type of fan control strategy, rough rice with higher MC required longer drying duration; the higher the air flowrate, the shorter the drying duration. The results (figure 4.6 (a), (b), and (c)) show that operating EMC-H fan control strategy resulted in the shortest drying duration while EMC-NA fan control strategy had the longest drying duration; the drying duration increased when the rough rice drying started late in the year. EMC-NA fan control strategy had the largest drying duration difference between different drying-start dates followed by CNA strategy, and EMC-H fan control strategy showed small difference between different drying-start dates. For example, for rough rice at IMC of 20%, drying using 0.69 m^3 $min\text{-}t^{-1}$ (0.5 cfm bu^{-1}) air flowrate resulted in drying duration of 42, 57, and 35 days when the drying was started on 15 August for CNA, EMC-NA, and EMC-H fan control strategies, respectively; but the same strategies resulted in drying durations of 44, 70, and 35 days for the 15 September and 55, 89, and 36 days for the 15 October drying-start dates, respectively. The reason was that EMC-NA and CNA fan control strategy were largely dependent on the weather conditions. The EMC-H fan control strategy allowed lowering the air EMC using heater, thereby lengthening the window of drying duration in a day.

For each type of fan control strategy, the rice with higher IMC suffered higher maximum DML, and the higher air flowrate reduced the maximum DML of rice in the bin. The maximum

DML of rice for different drying-start dates is shown in figure 4.7. The maximum DML decreased when the drying started later in the year under the same air flowrate, IMC, and fan control strategy (figure 4.7). For example, rough rice at IMC of 22% dried using EMC-H fan control strategy with 0.69 m^3 $min\text{-}t^{-1}$ (0.5 cfm bu^{-1}) air flowrate resulted in maximum DML of 0.37% when the drying started on 15 August, and the maximum DML reduced to 0.27% or 0.22% when the drying started one month or two months later, respectively. The reason could be that temperature plays a paramount role in the DML equation as expressed by Seib et al. (1980). Generally, temperature of air drops as winter approaches, and the respiration rates of rough rice and microorganism on rough rice drops as well; therefore, rough rice maintains lower DML when temperature is lower. For rough rice with the same IMC and dried in bins with the same height, air flowrate, and fan control strategy, drying duration was related to drying-start date, but rough rice maximum DML was inversely related to drying-start date. Also, DML in excess of 0.5% indicates the quality of rough rice depreciated and thus reduced grade value (USDA-FGIS, 1994). The rough rice with maximum DML is could be found on the top layer of the drying bed which remains at high rough rice MC for longer duration than the bottom layers.

The large standard deviations (SDs) of drying duration or maximum DML for each data in figures 4.6 and 4.7 were caused by yearly and geographic weather differences. Assuming the result is a normal distribution, 68.3% of values lie within one SD above or below the mean. For each fan control strategy, comparing SDs of drying duration and maximum DML between different drying strategy combinations, the magnitudes of SDs of drying duration or maximum DML and magnitudes of drying duration or maximum DML were directly related, respectively. For instance, similar to drying duration, SDs also decreased when IMC decreased, or air flowrate increased. Comparing the overall SDs of drying duration and maximum DML for different fan

control strategies, the EMC-H fan control strategy resulted in much smaller SDs compared to other two fan control strategies and led to smaller differences in the SDs between different IMCs, drying-start dates, and air flowrates (figures 4.6 and 4.7). The results of using EMC-H fan control strategy showed that the ranges of SD of drying duration and maximum DML were between 0.6 and 2.5 days, and 0.00% to 0.03%, respectively. In general, the variation in drying duration and maximum DML resulted from yearly and geographic weather differences; EMC-H fan control strategy showed the highest resistance to the weather difference compared to CNA and EMC-NA fan control strategies.

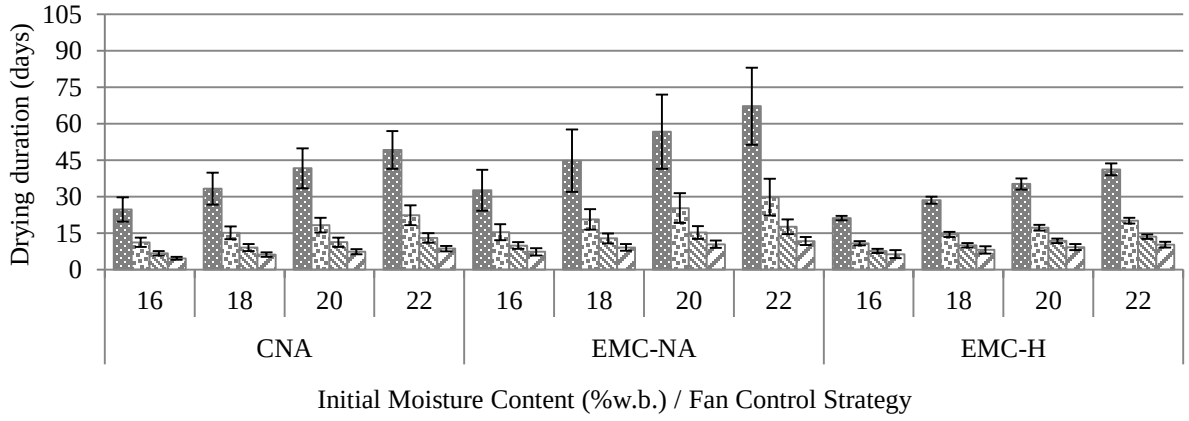

(a)

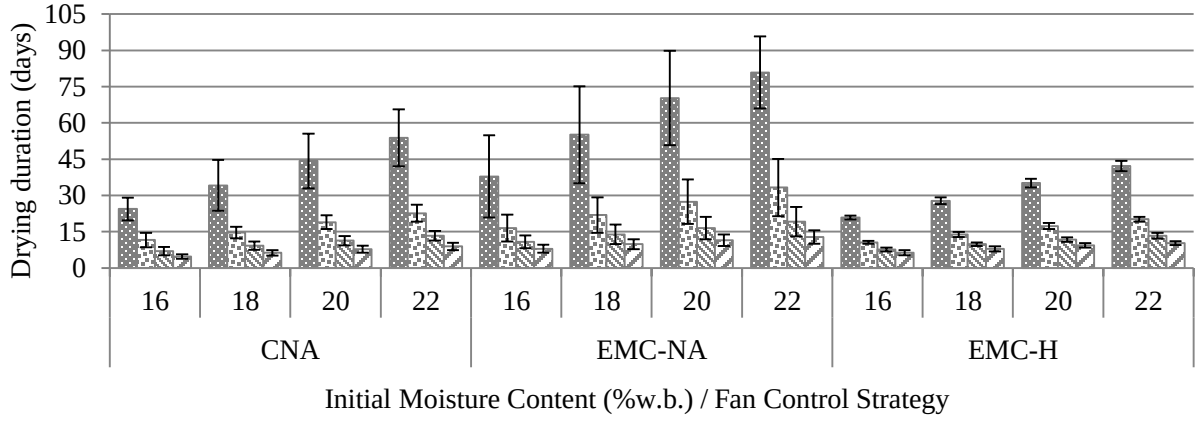

(b)

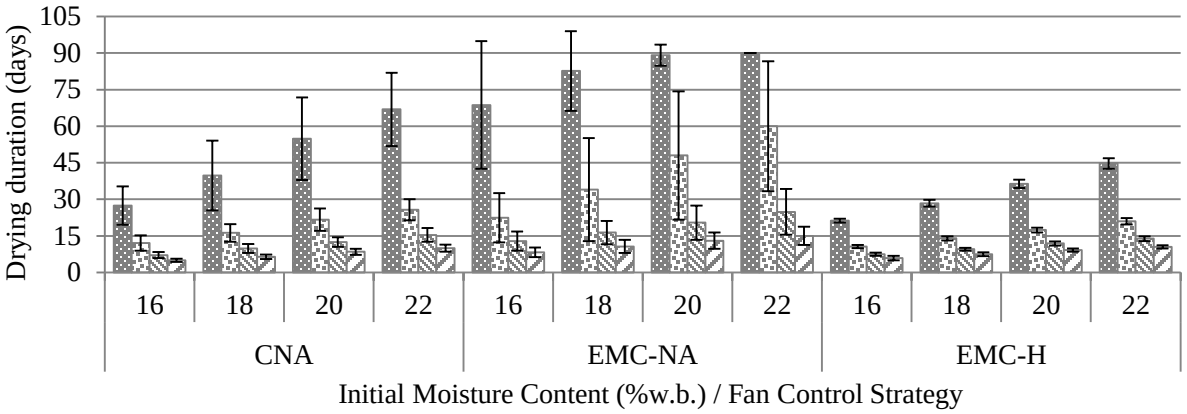

(c)

Figure 4.6. Effect of initial moisture content, fan control strategy (*CNA, EMC-NA, and EMC-H), air flowrate (▩ 0.69, ▩ 1.39, ▩ 2.08, and ▩ 2.77 m^3 $min\text{-}t^{-1}$), and drying-start date ((a) 15 August, (b) 15 September, and (c) 15 October) on rough rice drying duration. Each error bar was constructed using 1 standard deviation from the mean. *CNA – Continuous natural air fan control strategy; EMC-NA – Equilibrium moisture content controlled natural air fan control strategy; EMC-H – Equilibrium moisture content controlled air with supplemental heat fan control strategy.

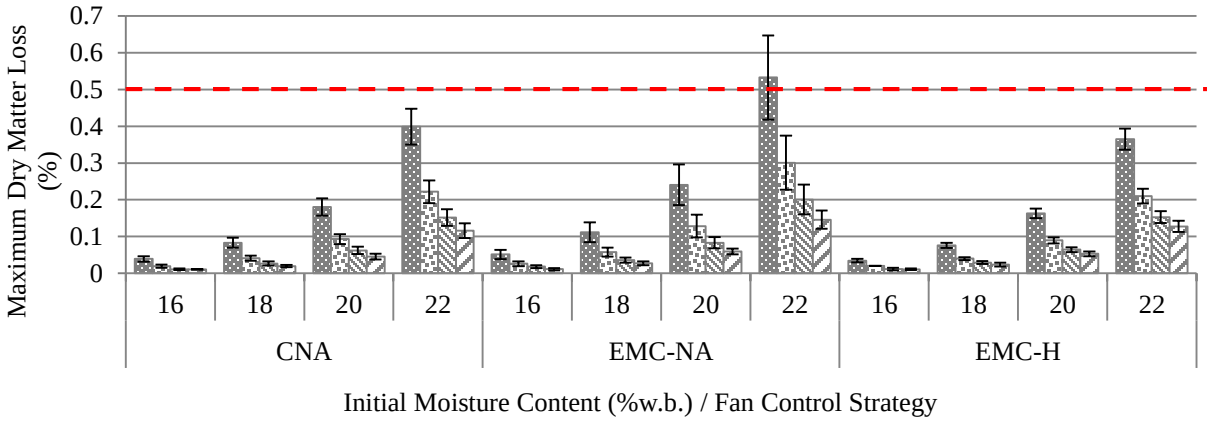

(a)

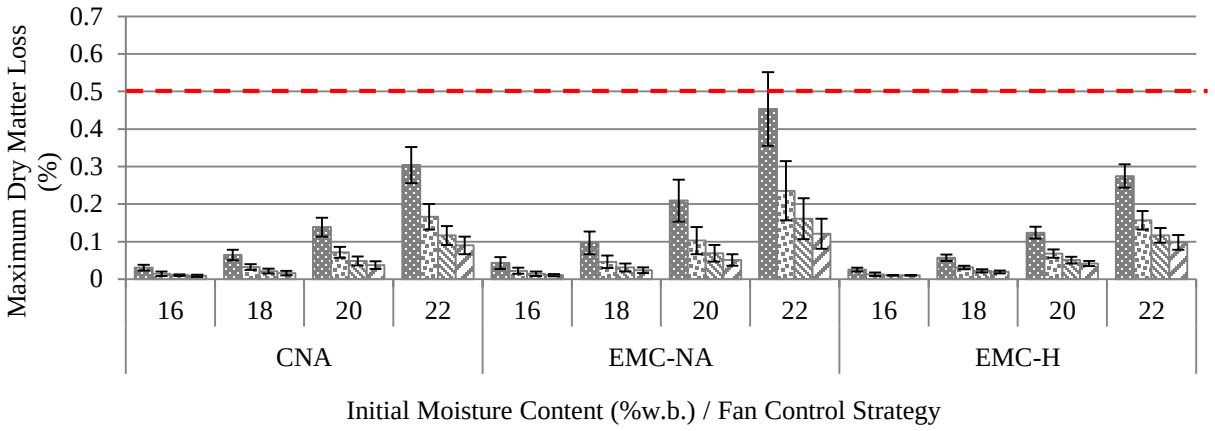

(b)

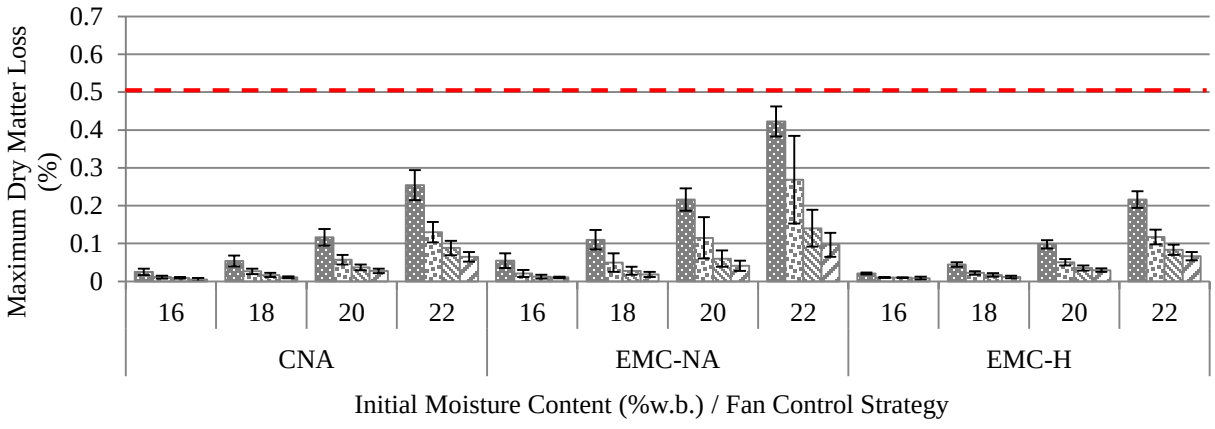

(c)

Figure 4.7. Effect of initial moisture content, fan control strategy (*CNA, EMC-NA, and EMC-H), air flowrate (▩ 0.69, ▩ 1.39, ▩ 2.08, and ▩ 2.77 m^3 $min\text{-}t^{-1}$), and drying-start date ((a) 15 August, (b) 15 September, and (c) 15 October) on rough rice maximum dry matter loss. Each error bar was constructed using 1 standard deviation from the mean. *CNA – Continuous natural air fan control strategy; EMC-NA – Equilibrium moisture content controlled natural air fan control strategy; EMC-H – Equilibrium moisture content controlled air with supplemental heat fan control strategy.

The effects of the studied drying strategies on minimum, maximum, and average final rough rice MC and percent overdrying of rough rice are shown in figure 4.8. The cross (×) and circular solid (●) marks represent the percent overdrying and the average final MC of the rough rice, respectively. The upper and lower limits of the solid box (▌) represent the average of the maximum and minimum final MCs attainable in the rough rice for the corresponding fan control

strategy, respectively. For example, in figure 4.8 (a) the simulations are performed with air flowrate of 0.69 m^3 $min\text{-}t^{-1}$ (0.5 cfm bu^{-1}); the left-most data of figure 4.8 (a) represents rough rice at IMC of 16%, drying from 15 August with fan control strategy set such that NA was continuously passed through the rough rice for 90 days or stopped earlier when rough rice in the top layer dried to a MC of 14%.

Based on the simulations, the feasibility to dry rough rice successfully, to the target MC, becomes questionable as the drying-start date delays from 15 August to 15 October, the air flowrate reduces from 2.77 m^3 $min\text{-}t^{-1}$ to 0.69 m^3 $min\text{-}t^{-1}$ (2.0 cfm bu^{-1} to 0.5 cfm bu^{-1}), and rough rice IMC increases from 16% to 22%, especially for EMC-NA fan control strategy (figure 4.8). For a normal distribution, there are about 32% of values lying outside of one SD above or below the mean. Thus, if the upper error bar of drying duration exceed 90 days, it indicates that top layer rough rice had at least 16% chance of not being able to dry completely, and the maximum final MC and possibly the average final MC of rough rice would exceed 14%. For example, rough rice with 20% or 22% IMC was not dried successfully when the drying started from 15 October using EMC-NA fan control strategy at air flowrate of 0.69 m^3 $min\text{-}t^{-1}$ as both average and maximum final MCs exceeded 14% (figure 4.8 (a)), and upper error bars of drying duration exceeded 90 days (figure 4.6 (c)). However, when CNA strategy was used, although upper error bars of drying duration were below 90 days in studied conditions (figure 4.6), figure 4.8 showed that all maximum final MCs were above 14% MC except in some cases when air flowrate was 2.77 m^3 $min\text{-}t^{-1}$ (2 cfm bu^{-1}); in some extreme cases, average final MCs were also above 14%. In the studied simulations, termination of the drying was executed when the top layer rough rice MC was 14% or after 90 days of drying. Evidently, the top layer rough rice MC was not the maximum final MC in the drying bed when CNA strategy was used. The reason for choosing top

layer rough rice MC to execute termination of simulation, instead of the highest MC layer of the whole rice bed, was because rice producers traditionally recognize that the drying operation would be completed when the top layer rough rice MC is lower than 14%. However, in actual practice, there is a possibility that air with high EMC may rewet the middle layer to exceed 14% MC when running fan continuously, as observed in the simulation results. Without the "cabling and sensing system" installed in the bin, the rice producers have no way to find out the MC of each layer of the rice bed. This problem may potentially result in rice quality reduction, especially for the under-dried rice layers at MC exceeding 14% MC.

In the simulations, the target average MC of rough rice was set at 13% to represent what the rice industry considers to be the safe short-term storage MC for rough rice (IRRI, 2010). The lower limit of rough rice MC (MC of 12%) was set to take into account the need to avoid shrinkage related costs, which bear negative economic consequences to producers. High percent overdrying represents high economical loss to the rice producers. High overdrying was observed in the rice bed only for conditions with fans operated under CNA strategy. When the simulations were conducted using CNA strategy at air flowrate of 0.69 m^3 $min\text{-}t^{-1}$ (0.5 cfm bu^{-1}), the percent overdrying increased, and the percent overdrying also increased. The maximum percent overdrying was 41.7% when rough rice with 22% IMC was dried from 15 September using CNA strategy at air flowrate of 2.77 m^3 $min\text{-}t^{-1}$ (2 cfm bu^{-1}). In some drying cases using CNA fan control strategy, the minimum final MC was larger than 12%, but the percent overdrying was larger than zero. For example, when rough rice with 22% IMC was dried from 15 August using CNA strategy at air flowrate of 1.39 m^3 $min\text{-}t^{-1}$ (1 cfm bu^{-1}), the resulting minimum final MC was 12.4% and the percent overdrying was 8.6%. This could be explained by the fact that the minimum final MCs and percent overdrying represent average of data obtained after individual

simulations which used a total of 20 years (1995-2014) of weather data at five locations; there might be a need to design drying guidelines by considering location-related effects.

For EMC-NA or EMC-H fan control strategies, when both the bottom layer rough rice MC and plenum air EMC are above the set EMC high limit (14% MC), the control system would stop the fan operation or turn on the heater, respectively. Therefore, once a layer in the rice bed is dried below 14% MC, the layer cannot be rewetted to exceed 14% MC. Thus, the top layer rough rice has the maximum final MC in the bin and is the last layer to dry to 14% MC. Also, the fan-operation window narrows as the rough rice MC approaches the targeted EMC (equation 11). For EMC-H and EMC-NA fan control strategies, the fan operation stops when both the bottom layer rough rice MC and plenum air EMC are less than the set EMC low limit; air which could overdry the rough rice is not permitted into the bin through the rice when the average rough rice MC is close to the targeted MC. Therefore, percent overdryings were nearly zero for all studied conditions when the fan was operated under the EMC-H and EMC-NA strategies (figure 4.8). The dynamic EMC low limit are regulated such that at the beginning, the bottom layer of grain was slightly overdried (equation 11); as the drying front moves to the top, the rice in the bottom layer slightly rewets and progressively and slowly increases to 12% MC. Ideally, the dynamic EMC low limit will speed up the drying duration. In actual operation, the success of dynamic EMC low limit is depended on the accuracy of the sensors, and sensor failure may cause significant overdrying or rewetting of the bottom layer of rice. Therefore, dynamic EMC low limit is often implemented manually in actual field scenarios. For example, the set EMC low limit of bin A was manually changed from 8.5% to 9.5% to 10.5% MCs as the drying progressed (table 3.2).

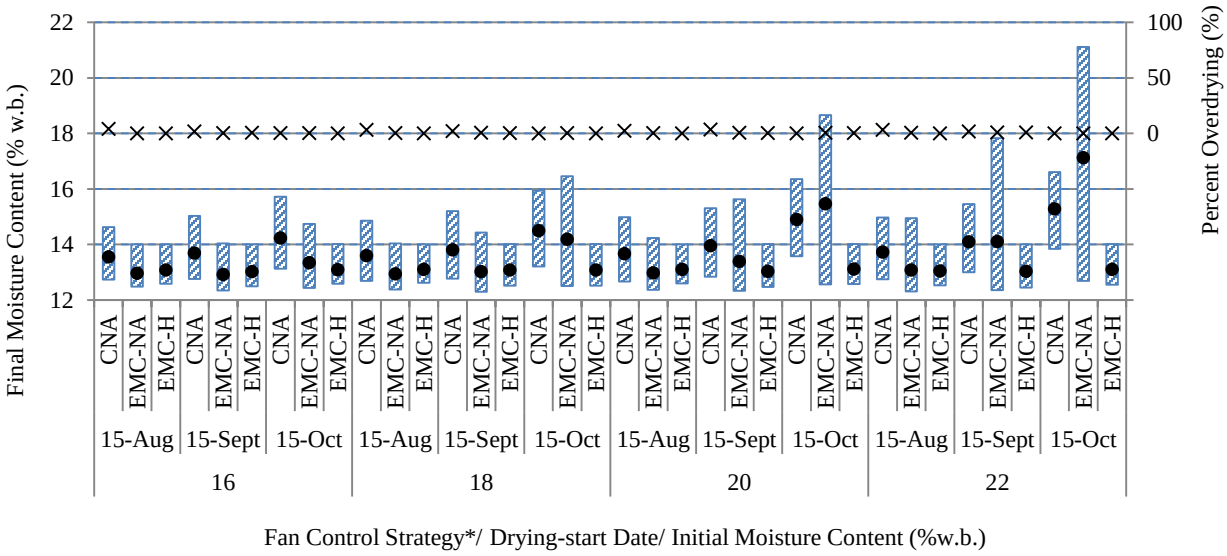
Final Moisture Content (% w.b.)
Percent Overdrying (%)
22
20
18
16
14
12
100
50
0
CNA
EMC-NA
EMC-H
15-Aug
15-Sept
15-Oct
16
18
20
22
Fan Control Strategy*/ Drying-start Date/ Initial Moisture Content (%w.b.)

(a)

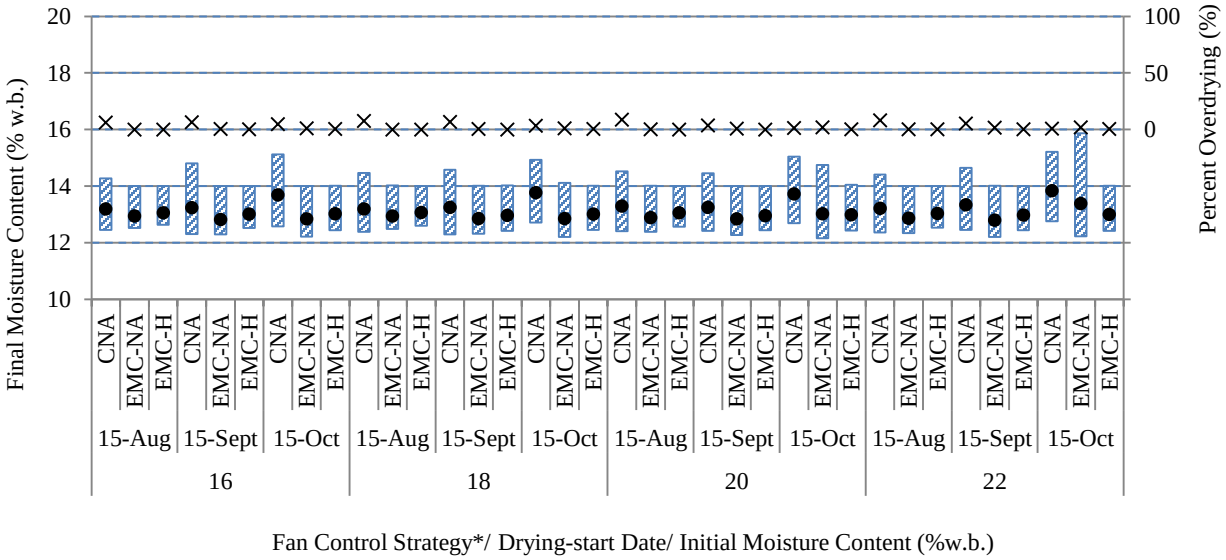
Final Moisture Content (% w.b.)
Percent Overdrying (%)
20
18
16
14
12
10
100
50
0
CNA
EMC-NA
EMC-H
15-Aug
15-Sept
15-Oct
16
18
20
22
Fan Control Strategy*/ Drying-start Date/ Initial Moisture Content (%w.b.)

(b)

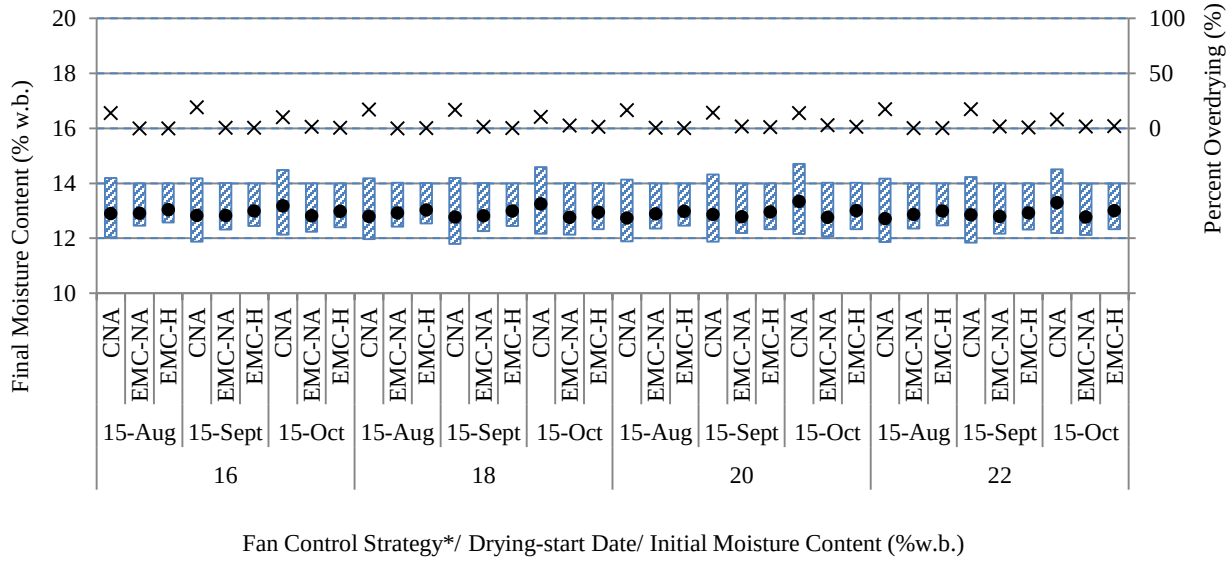

(c)

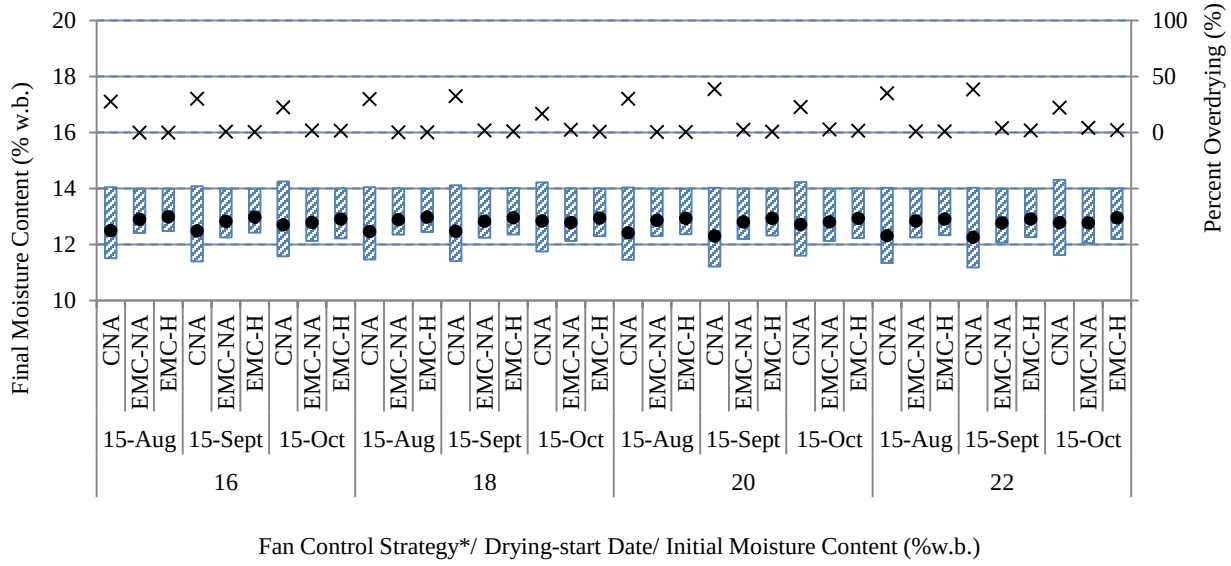

(d)

Figure 4.8. Effects of initial moisture content, fan control strategy, drying-start date, and air flowrate ((a) 0.69 m^3 $min\text{-}t^{-1}$ (0.5 cfm bu^{-1}), (b) 1.39 m^3 $min\text{-}t^{-1}$ (1 cfm bu^{-1}), (c) 2.08 m^3 $min\text{-}t^{-1}$ (1.5 cfm bu^{-1}), and (d) 2.77 m^3 $min\text{-}t^{-1}$ (2 cfm bu^{-1})) on percent overdrying (right Y-axis) and minimum, maximum, and average final moisture content of rough rice (left Y-axis); The cross (×) and circular solid (●) marks represent the percent overdrying and the average final MC of the rice bed, respectively. The upper and lower limits of the solid box (▌) represent the average of the maximum and minimum final MCs attainable in the rice bed. *CNA – Continuous natural air fan control strategy; EMC-NA – Equilibrium moisture content controlled natural air fan control strategy; EMC-H – Equilibrium moisture content controlled air with supplemental heat fan control strategy.

5. CONCLUSION AND FUTURE RESEARCH

5.1 Equilibrium moisture content determination

Adsorption and desorption isotherms of long-grain hybrid rough rice (cultivar CL XL745) were determined, and the result showed the average desorption EMC was higher than average adsorption EMC, and rough rice EMC significantly increased when air temperature decreased, or air RH increased. Four empirical EMC models (modified Chung-Pfost, modified Halsey, modified Henderson, and modified Oswin) were fitted with actual data, and constants for predicting both adsorption and desorption EMCs were established. The modified Halsey and modified Chung-Pfost equations best predicted EMCs of long-grain hybrid rough rice for adsorption and desorption conditions, respectively. The modified Chung-Pfost equation and associated adsorption and desorption constants were selected for the simulation study.

5.2 Simulations for model validation

On-farm, in-bin drying systems, equipped with sensors for automatic monitoring of grain temperature and RH in the bin, were used to validate a developed model for NA, in-bin drying of rough rice in Arkansas locations. Rough rice MC data determined by field sensors over-predicted the meter-measured MCs by 4.54% and 7.60%, and the RMSEs were 1.48% MC and 0.73% MC for drying bins located at Burdette and Dermott, Arkansas, respectively. The slight difference between results from field sensors and moisture meter measurements may be attributed to (1) variation of sampling points relative to the sensor position, (2) the accuracy of prediction of temperature and RH by the sensors, and (3) accuracy of the equation used to calculate the rough rice MC from the temperature and RH data.

Simulation results of rough rice MC and temperature from the developed model were compared with field sensor-determined profiles for rough rice drying with EMC-NA fan control strategy. The mean RMSEs of rough rice MC and temperature were less than 0.57 ±0.10% MC and 1.91 ±0.21 ℃, respectively; mean NSEs of rough rice MC and temperature were greater than 0.68 ±0.50 and 0.49 ±0.04, respectively; PBIAS range of rough rice MC were between -3.53% and 5.76%; PBIAS range of rough rice temperature were between -3.96% and 1.78%. These statistical parameters indicated that the simulated rough rice MC and temperature profiles predicted well the rough rice temperature and MC data, determined using field sensors.

5.3 Simulations to assess impacts of in-bin rough rice drying strategies

The implications of fan control strategies, IMC, drying-start date, and air flowrate on in-bin drying of rough rice at Jonesboro, West Memphis, and Stuttgart in Arkansas, and Greenville and Tunica in Mississippi were investigated. Drying simulations were performed using the PHAST-FDM model which was modified for rice. The simulations provided useful information to guide rice producers achieve successful rice drying. For example, figure 5.1 illustrates the critical operation ranges for various drying strategies that will limit rice drying within one month while maintaining maximum DML and percent overdrying equal to or lower than 0.5% and 10%, respectively.

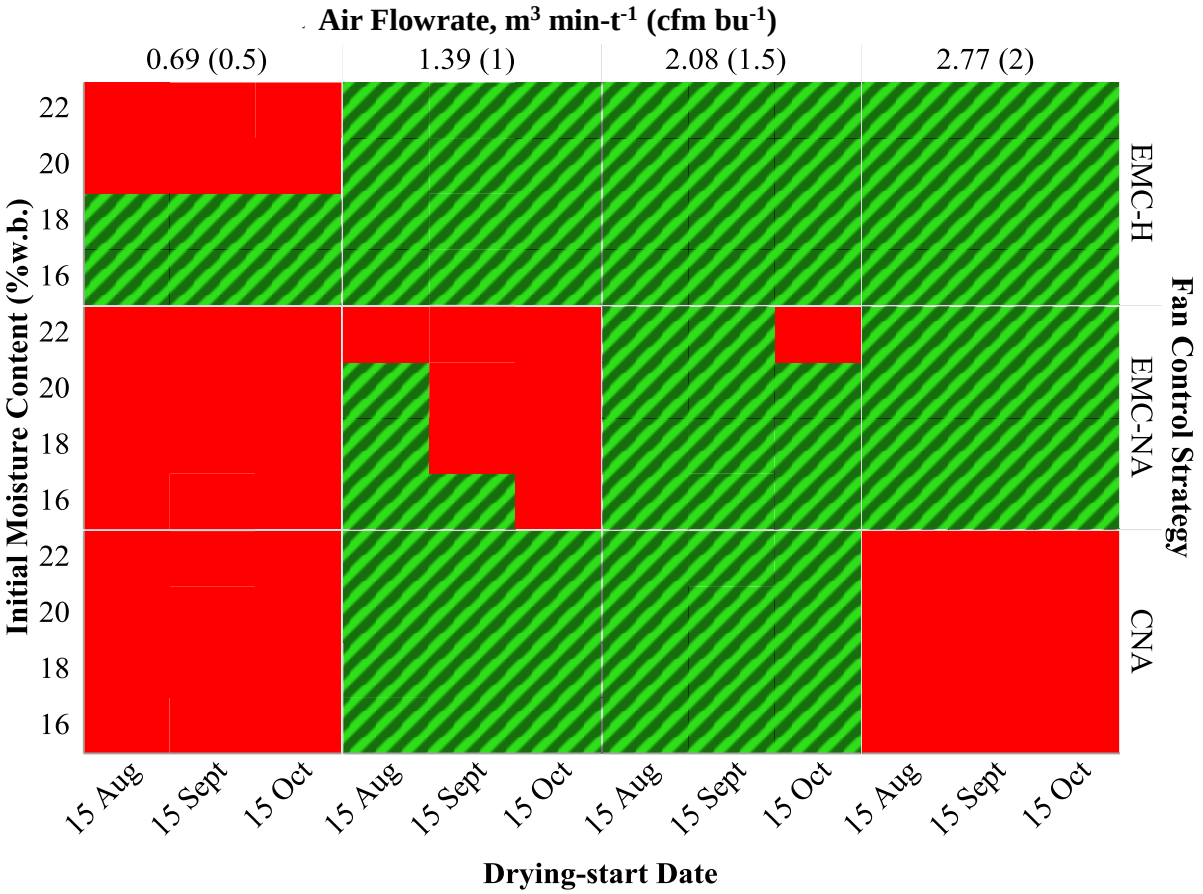

Figure 5.1. Critical operation ranges for various drying strategies including initial moisture content (16%, 18%, 20%, and 22%w.b.), fan control strategy (*CNA, EMC-NA, and EMC-H), air flowrate (0.69, 1.39, 2.08, and 2.77 m^3 $min\text{-}t^{-1}$), and drying-start date (15 August, 15 September, and 15 October), that will limit rough rice drying within one month while maintaining DML and percent overdrying of equal or lower than 0.5% and 10%, respectively. The green squares with diagonal stripes (▨) represent the suitable drying operation range, and the red squares with no diagonal stripes (■) represent the unsuitable drying operation range. *CNA – Continuous natural air fan control strategy; EMC-NA – Equilibrium moisture content controlled natural air fan control strategy; EMC-H – Equilibrium moisture content controlled air with supplemental heat fan control strategy.

In general, EMC-H fan control strategy for in-bin drying of rough rice had the fastest drying rate, low percent overdrying, and high resistance to yearly and geographic weather differences (i.e. compared to other two fan control strategies); therefore, the drying duration and maximum DML were relatively consistent year by year. EMC-NA fan control strategy resulted in slower drying rate, low percent overdrying, and lower resistance to yearly and geographic

weather differences; therefore, the drying duration and maximum DML varied year by year. Compared to EMC-NA fan control strategy, using CNA fan control strategy would be slightly faster and have slightly better weather resistance in terms of drying duration and maximum DML; however, the CNA may bear three disadvantages: (1) high percent overdrying, (2) negative quality impacts caused by rice overdrying and rewetting, and (3) potential safety concerns of mold growth leading to formation of mycotoxin.

5.4 Future studies

In future, very carefully controlled lab and field studies that simulate in-bin rough rice drying are recommended to determine the kinetics of grain quality reduction. The determined results should be integrated in the models developed to provide robust results. Such results should address the kinetics of head rice yield reduction, rice discoloration, mold growth, and formation of mycotoxins. While conducting such experiments in the field, the following should be considered to obtain useful results: (1) implications of common cultural practices such as bin coring, bin leveling, comingling of rice, use of grain spreader, levels of MOGs in rice, and harvesting methods; and (2) year by year climate changes which may affect the choice of drying strategy in a specific location.

REFERENCES

Agrawal, A. M., Manek, R. V., Kolling, W. M., & Neau, S. H. (2004). Water distribution studies within microcrystalline cellulose and chitosan using differential scanning calorimetry and dynamic vapor sorption analysis. *Journal of Pharmaceutical Sciences*, 93(7), 1766-1779.

Ambardekar, A. A., & Siebenmorgen, T. J. (2012). Effects of postharvest elevated-temperature exposure on rice quality and functionality. *Cereal Chemistry*, 89(2), 109-116.

Aregba, A. W., & Nadeau, J. P. (2007). Comparison of two non-equilibrium models for static grain deep-bed drying by numerical simulations. *Journal of Food Engineering*, 78(4), 1174-1187.

ASABE Standards. (2011). *D272.3 Resistance to airflow of grains, seeds, other agricultural products and perforated metal sheets.* St. Joseph, Mich.: ASABE.

ASABE Standards. (2012). *D245.6 Moisture relationships of plant-based agricultural products.* St. Joseph, Mich.: ASABE.

ASABE Standards. (2014). *D271.2 Psychrometric Data.* St. Joseph, Mich.: ASABE.

ASAE Standards. (2006). *ASAE S352.2 Moisture Measurement--Unground Grain and Seeds.* St. Joseph, Mich.: ASAE.

Atungulu, G. G., Zhong, H., Thote, S., Okeyo, A., & Couch, A. (2015). Microbial Prevalence on Freshly-harvested Long-grain Pureline, Hybrid and Medium-grain Rice Cultivars. *Applied Engineering in Agriculture*.

Banaszek, M. M., & Siebenmorgen, T. J. (1990). Head rice yield reduction rates caused by moisture adsorption. *Transactions of the ASAE*, 33(4), 1263-1269.

Barre, H. J., Baughman, G. R., & Hamdy, M. Y. (1971). Application of the logarithmic model to cross-flow deep-bed grain drying. *Transactions of the ASAE*, 14(6), 1061-1064.

Bartosik, R. E., & Maier, D. E. (2004). Evaluation of three NA/LT in-bin drying strategies in four Corn Belt locations. *Transactions of the ASABE*, 47(4), 1195-1206.

Baumgartner, S., Kristl, J., & Peppas, N. A. (2002). Network structure of cellulose ethers used in pharmaceutical applications during swelling and at equilibrium. *Pharmaceutical Research*, 19(8), 1084-1090.

Bingol, G., Prakash, B., & Pan, Z. (2012). Dynamic vapor sorption isotherms of medium grain rice varieties. *LWT-Food Science and Technology*, 48(2), 156-163.

Bloome, P. D., & Shove, G. C. (1971). Near equilibrium simulation of shelled corn drying. *Transactions of the ASAE*, 14(4), 709-0712.

Boac, J. M., Casada, M. E., Maghirang, R. G., & Harner III, J. P. (2010). Material and interaction properties of selected grains and oilseeds for modeling discrete particles. *Transactions of the ASABE*, 53(4), 1201-1216.

Brooker, D., Bakker-Arkema, F., & Hall, C. (1992). *Drying and Storage of Grains and Oilseeds.* New York: AVI Van Nostrand Reinhold.

Choi, B., Lanning, S. B., & Siebenmorgen, T. J. (2010). A review of hygroscopic equilibrium studies applied to rice. *Transactions of the ASABE*, 53(6), 1859-1872.

Cnossen, A. G., & Siebenmorgen, T. J. (2000). The glass transition temperature concept in rice drying and tempering: Effect on milling quality. *Transactions of the ASAE*, 43(6), 1661-1668.

Cnossen, A. G., Siebenmorgen, T. J., Yang, W., & Bautista, R. C. (2001). An application of glass transition temperature to explain rice kernel fissure occurrence during the drying process. *Drying Technology*, 19(8), 1661-1682.

Ekechukwu, O. V., & Norton, B. (1999). Review of solar-energy drying systems II: an overview of solar drying technology. *Energy Conversion and Management*, 40(6), 615-655.

Guillard, V., Broyart, B., Bonazzi, C., Guilbert, S., & Gontard, N. (2003). Moisture diffusivity in sponge cake as related to porous structure evaluation and moisture content. *Journal of Food Science*, 68(2), 555-562.

Gupta, H. V., Sorooshian, S., & Yapo, P. O. (1999). Status of automatic calibration for hydrologic models: Comparison with multilevel expert calibration. *Journal of Hydrologic Engineering*, 4(2): 135-143.

Hogan, S. E., & Buckton, G. (2001). The application of near infrared spectroscopy and dynamic vapor sorption to quantify low amorphous contents of crystalline lactose. *Pharmaceutical Research*, 18(1), 112-116.

Iguaz, A., & Virseda, P. (2007). Moisture desorption isotherms of rough rice at high temperatures. *Journal of Food Engineering*, 79(3), 794-802.

Inprasit, C., & Noomhorm, A. (2001). Effect of drying air temperature and grain temperature of different types of dryer and operation on rice quality. *Drying Technology*, 19(2), 389-404.

IRRI. (2010). Measuring Rice Moisture Content.

Jindal, V. K., & Siebenmorgen, T. J. (1987). Effects of oven drying temperature and drying time on rough rice moisture content determination. *Transactions of the ASAE*, 30(4), 1185-1192.

Jindal, V. K., & Siebenmorgen, T. J. (1994). Simulation of low temperature rough rice drying and rewetting in shallow beds. *Transactions of the ASAE*, 37(3), 863-871.

Lawrence, J., Atungulu, G., & Siebenmorgen, T. (2015). Modeling in-bin rice drying using natural air and controlled air drying strategies. *Transactions of the ASABE*, 58(4), 1103-1111.

Mittal, G. S., & Otten, L. (1982). Simulation of low temperature corn drying. *Canadian Agricultural Engineering*, 24(2), 111-118.

Nash, J., & Sutcliffe, J. V. (1970). River flow forecasting through conceptual models part I—A discussion of principles. *Journal of Hydrology*, 10(3), 282-290.

Ondier, G. O., Siebenmorgen, T. J., & Mauromoustakos, A. (2010). Low-temperature, low-relative humidity drying of rough rice. *Journal of Food Engineering*, 100(3), 545-550.

Ondier, G. O., Siebenmorgen, T. J., Bautista, R. C., & Mauromoustakos, A. (2011). Equilibrium moisture contents of pureline, hybrid and parboiled rice. *Transactions of ASABE*, 53(3), 1007-1013.

Pabis, S., Jayas, D. S., & Cenkowski, S. (1998). *Grain drying: Theory and practice.* John Wiley & Sons.

Richard, J. L., Payne, G. E., Desjardins, A. E., Maragos, C., Norred, W. P., & Pestka, J. J. (2003). Mycotoxins: risks in plant, animal and human systems. *CAST Task Force Report*, 139, 101-103.

Roman-Gutierrez, A. D., Mabille, F., Guilbert, S., & Cuq, B. (2003). Contribution of specific flour components to water vapor adsorption properties of wheat flours. *Cereal Chemistry*, 80(5), 558-563.

Sahay, M. N., & Gangopadhyay, S. (1985). Effect of wet harvesting on biodeterioration of rice. *Cereal Chemistry*, 62(2), 80-83.

Saksena, V., Montross, M. D., & Maier, D. E. (1998). NA/LT drying strategies for white corn in two corn belt locations. *ASAE Paper No. 986049. St. Joseph, Mich.: ASAE.*

Schluterman, G. J., & Siebenmorgen, T. J. (2004). Air and rice property profiles within a commercial cross-flow rice dryer. *Applied Engineering in Agriculture*, 20(4), 487-494.

Seib, P. A., Pfost, H. B., Sukabdi, A., Rao, V. G., & Burroughs, R. (1980). Spoilage of rough rice measured by evolution of carbon dioxide. *Grain Quality Improvement: Proceedings of 3rd Annual Workshop on Grains Post-harvest Technology*, (pp. 75-94). Kuala Lumpur.

Sharma, S. C., & Muir, W. (1974). Simulation of heat and mass transfer during ventilation of wheat and rapeseed bulks. *Canadian Agricultural Engineering*, 16(1).

Sharp, J. R. (1982). A review of low temperature drying simulation models. *Journal of Agricultural Engineering Research*, 27(3), 169-190.

Siebenmorgen, T. J., & Jindal, V. K. (1986). Effects of moisture adsorption on the head rice yields of long-grain rough rice. *Transactions of the ASAE*, 29(6): 1767-1771.

Singh, C. B., Jayas, D. S., & Larson, R. (2014). Assessment of fan control strategies for in-bin natural air-drying of wheat in Western Canada. *Canadian Biosystems Engineering*, 56.

Soponronnarit. (1988). Energy model of grain drying system. *ASEAN Journal on Science and Technology for Development*, 5(2), 43-68.

Srivastava, V. K., & John, J. (2002). Deep bed grain drying modeling. *Energy Conversion and Management*, 43(13), 1689-1708.

Sun, D. W. (1999). Comparison and selection of EMC/ERH isotherm equations for rice. *Journal of Stored Products Research*, 35(3), 249-264.

Teoh, H. M., Schmidt, S. J., Day, G. A., & Faller, J. F. (2001). Investigation of cornmeal components using dynamic vapor sorption and differential scanning calorimetry. *Journal of Food Science*, 66(3), 434-440.

Thompson, T. L. (1972). Temporary storage of high-moisture shelled corn using continuous aeration. *Transactions of the ASAE*, 15(2), 333-337.

Tirawanichakul, Y., Prachayawarakorn, S., Tungtrakul, P., Chaiwatpongskorn, W., & Soponronnarit, S. (2003). Experiments on in-store paddy drying under tropical climate: simulation and product quality. *Drying Technology*, 21(6), 1049-1064.

USDA-FGIS (US Department of Agriculture-Federal Grain Inspection Service). (1994). *Rice Inspection Handbook.* Washington, DC.

Young, P. M., Chiou, H., Tee, T., Traini, D., Chan, H. K., Thielmann, F., & Burnett, D. (2007). The use of organic vapor sorption to determine low levels of amorphous content in processed pharmaceutical powders. *Drug Development and Industrial Pharmacy*, 33(1), 91-97.